

# The role of aneuploidy in the evolution of cancer drug resistance

Remus Stana<sup>1</sup>, Uri Ben-David<sup>2</sup>, Daniel B. Weissman<sup>3</sup>, and Yoav Ram<sup>1,\*</sup>

<sup>1</sup>School of Zoology, Faculty of Life Sciences, Tel Aviv University, Tel Aviv, Israel

<sup>2</sup>Department of Human Molecular Genetics and Biochemistry, Faculty of Medicine, Tel Aviv University, Tel Aviv, Israel

<sup>3</sup>Department of Physics, Emory University, Atlanta, GA

\*Corresponding author: yoav@yoavram.com

February 2, 2024

## Abstract

Evolutionary rescue is the process by which a population survives a sudden environmental change that initially causes the population to decline towards extinction. A prime example of evolutionary rescue is the ability of cancer to survive exposure to various treatments. One evolutionary mechanism by which a population of cancer cells can adapt to chemotherapy is aneuploidy. Aneuploid cancer cells can have higher fitness in an environment altered by anti-cancer drugs, e.g., because of incomplete pathways targeted by the drugs. Indeed, aneuploidy is highly prevalent in tumors, and moreover, some anti-cancer drugs fight cancer by increasing chromosomal instability. Here, we examine how aneuploidy impacts the fate of a population of cancer cells. We use multi-type branching processes to approximate the probability that a tumor survives drug treatment as a function of the initial tumor size, and rates at which aneuploidy and other beneficial mutations occur, and the growth rates of the sensitive and resistant cells. We also approximate the mean recurrence time for the tumor to revert back to its initial size. We find that aneuploidy can play an important role in the relapse of secondary tumors who have not yet been detected and thus are smaller in size.

Keywords: whole-chromosome duplication, evolutionary model, adaptive evolution, cancer, drug resistance, chromosome instability

# Introduction

**Aneuploidy in cancer.** Each year approximately 10 million people die from cancer (Kocarnik et al., 2022), so understanding the factors that contribute to failure of interventions is of great importance. One hypothesized factor is aneuploidy, where cells are characterized by an imbalanced karyotype and chromosome copy number alterations (Schukken and Foijer, 2018), caused by chromosomal instability (CIN), the mitotic process in which cells suffer from chromosome mis-segregation that leads to aneuploidy. Importantly, aberrations in chromosome copy number have been shown to allow cancer cells to survive under stressful conditions such as drug therapy (Lukow et al., 2021, Rutledge et al., 2016). Indeed, cancer cells are often likely to be aneuploid, and aneuploidy is associated with poor patient outcomes (Ben-David and Amon, 2020, Smith and Sheltzer, 2018).

Ippolito et al. (2021) induced aneuploidy in cancer cell lines by exposing them to reversine, a small-molecule inhibitor of the mitotic kinase Mps1, and then to chemotherapeutic agents such as vemurafenib. Reversine-treated cells had higher proliferation rate in the environment altered by anti-cancer drugs compared to wildtype cancer cells. Similarly, Lukow et al. (2021) induced aneuploidy in cancer cells and observed that such cells have an advantage compared to wildtype cells during chemotherapy, despite having lower fitness before the onset of chemotherapy. One proposed mechanism through which aneuploidy is able to confer resistance to chemotherapeutics is by antagonizing cell division, which prevents the drugs from damaging DNA and microtubules (Replogle et al., 2020).

An important aspect of aneuploidy is the rate with which cells become aneuploid, which is several orders of magnitude higher than the beneficial mutation rate (Bakker et al., 2023). Consequently, a cell exposed to a stress such as chemotherapeutic drugs can acquire aneuploidy faster when compared to acquiring a mutation, especially when several proposed anti-cancer drugs elevate the rate of mis-segregation in order to fight cancer (Lee et al., 2016).

**Evolutionary rescue.** Populations adapted to a certain environment are vulnerable to environmental changes, which might cause extinction of the population. Examples of such environmental changes include climate change, invasive species or the onset of drug therapies. Adaptation is a race against time as the population size decreases in the new environment (Tanaka and Wahl, 2022). *Evolutionary rescue* is the process where the population acquires a trait that increases fitness in the new environment such that extinction is averted. It is mathematically equivalent to the problem of crossing of fitness valley (Weissman et al., 2009, 2010). There are three potential ways for a population to survive environmental change: migration to a new habitat similar to the one before the onset of environmental change (Cobbold and Stana, 2020, Harsch et al., 2014, Zhou, 2022); adaptation by phenotypic plasticity without genetic modification (Carja and Plotkin, 2017, 2019, Gunnarsson et al., 2020, Levien et al., 2021); and adaptation through genetic modifications, e.g., mutation (Gomulkiewicz and Holt, 1995, Orr and Unckless, 2014, Uecker and Hermisson, 2011, 2016, Uecker et al., 2014).

Gunnarsson et al. (2020) analyze a model where a tumor consisting of two populations of cancer cells, one drug resistant and the other drug sensitive, is able to evade extinction by cells switching between the two phenotypes through epigenetic mutations. They found that even when the drug resistant type is barely viable the epimutations have the effect of guaranteeing evolutionary rescue. Evolutionary rescue in one step in which an initially declining population, after a sudden environmental change, has to acquire a mutation has been studied in the context of population genetics by (Orr and Unckless, 2008, 2014). They analyzed a model where the mutant strain is present in small number at the onset of therapy and concluded that this can significantly enhance the chance that the population will survive.

Most models focus on the probability that at least one mutation rescues the population. How multiple mutations contribute to the survival of the population is less explored, but Wilson et al. (2017) have shown that evolutionary rescue is significantly enhanced by soft selective sweeps when

multiple mutations contribute. Evolutionary rescue that requires two successive mutations has been investigated using diffusion approximation by Martin et al. (2013).

Here we build on previous work on evolutionary rescue after a sudden environment change caused by the initiation of chemotherapy. We wish to understand what effect does aneuploidy have on the probability of evolutionary rescue when it acts as an intermediary between the wildtype and the mutant cancer cells. We also calculate the mean time that an initially declining tumor cell population reaches its pre-treatment size. Given that aneuploidy is present in many tumors even before the onset of therapy (Lukow et al., 2021) we also take into consideration the effect that standing genetic variation has on the tumor dynamics.

## Methods

### Evolutionary model

We follow the number of cancer cells that have one of three different genotypes at time  $t$ : wildtype,  $w_t$ ; aneuploid,  $a_t$ ; and mutant,  $m_t$ . These cells divide and die with rates  $\lambda_k$  and  $\mu_k$  (for  $k = w, a, m$ ). The difference between the division and death rate is  $\Delta_k = \lambda_k - \mu_k$ . We assume the population of cells is under a strong stress, such as drug therapy, to which the wildtype genotype is susceptible or sensitive and therefore  $\Delta_w < 0$ , whereas the mutant is resistant to the stress,  $\Delta_m > 0$ . We analyze three scenarios: in the first, aneuploid cells are partially resistant,  $\Delta_m > \Delta_a > 0$ ; in the second, aneuploid cells are tolerant,  $0 > \Delta_a > \Delta_w$  (see Brauner et al., 2016, for the distinction between susceptible, resistant, and tolerant); in the third, aneuploid cells are non-growing, stationary or "barely growing", that is, either slightly tolerant or slightly resistant, such that  $\Delta_a \approx 0$ . We assume that both chromosomal missegregation and mutation occur during the process of mitosis. Wildtype cells may divide and then missegregate to become aneuploids at rate  $u\lambda_w$ . Both aneuploid and wildtype cells may divide and mutate to become mutants at rates  $v\lambda_a$  and  $v\lambda_w$ , respectively. See Figure 1 for a schematic representation of the model and Figure 2 for sample trajectories of the different genotypes for  $u = 0$  (A),  $\Delta_a \ll 0$  (B),  $\Delta_a \approx 0$  (C),  $\Delta_a \gg 0$  (D). We assume that wildtype cells acquire aneuploidy before the onset of therapy with rate  $\tilde{u}\lambda_w$  and that aneuploid cells have a fitness cost  $s$  in the drug-free environment.

### Stochastic simulations

Simulations are performed using a *Gillespie algorithm* (Gillespie, 1976, 1977) implemented in Python (Van Rossum and Others, 2007). The simulation monitors the number of cells of each type: wildtype, aneuploid, and mutant. The wildtype population initially consists of  $w_0 = N$  cells, whereas the other cell types are initially absent.

The state of the stochastic system at time  $t$  is represented by the triplet  $(w_t, a_t, m_t)$ . The following describes the events that may occur (right column), the rates at which they occur (middle column), and the effect these events have on the state (left column, see Figure 1):

$$\begin{aligned}
(+1, 0, 0) : & \quad \lambda_w w_t (1 - u - v) \quad (\text{birth of wildtype cell}) , \\
(-1, 0, 0) : & \quad \mu_w w_t \quad (\text{death of wildtype cell}) , \\
(0, +1, 0) : & \quad u\lambda_w w_t \quad (\text{wildtype cell divides and becomes aneuploid}) , \\
(0, 0, +1) : & \quad v\lambda_w w_t \quad (\text{wildtype cell divides and becomes mutant}) , \\
(0, +1, 0) : & \quad \lambda_a a_t (1 - v) \quad (\text{birth of aneuploid cell}) , \\
(0, -1, 0) : & \quad \mu_a a_t \quad (\text{death of aneuploid cell}) , \\
(0, 0, +1) : & \quad v\lambda_a a_t \quad (\text{aneuploid cell divides and becomes mutant}) ,
\end{aligned}$$

$$\begin{aligned}
(0, 0, +1) : & \quad \lambda_m m_t \quad (\text{birth of mutant cell}), \\
(0, 0, -1) : & \quad \mu_m m_t \quad (\text{death of mutant cell}).
\end{aligned}$$

For the remaining of this paper we assume that the division rates for wildtype and aneuploid cells can be written as  $\lambda_w w_t (1 - u - v) \approx \lambda_w w_t$  and  $\lambda_a a_t (1 - v) \approx \lambda_a a_t$  because  $u, v \ll 1$  (see Table 1). Each iteration of the simulation loop starts with computing the rates  $v_j$  of each event  $j$ . We then draw the time until the next event,  $\Delta t$ , from an exponential distribution whose rate parameter is the sum of the rates of all events, such that  $\Delta t \sim \text{Exp}(\sum_j v_j)$ . Then, we randomly determine which event occurred, where the probability for event  $j$  is  $p_j = v_j / \sum_i v_i$ . Finally, we update the number of cells of each type according to the event that occurred and update the time from  $t$  to  $t + \Delta t$ . We repeat these iterations until either the population becomes extinct (the number of cells of all types is zero) or the number of mutant cells is high enough so that its extinction probability is  $< 0.1\%$ , that is until

$$m_t > \left\lceil \frac{3 \log 10}{\log(\lambda_m / \mu_m)} \right\rceil + 1.$$

where we obtain the threshold mutant size by solving  $1 - (1 - p_m)^{m_t} = 0.999$  for  $m_t$ , where  $p_m = \Delta_m / \lambda_m$  is the probability that a single mutant escapes stochastic extinction (see Appendix A).

**$\tau$ -leaping.** When simulations are slow (e.g. due to large population size), we utilize  $\tau$ -leaping (Gillespie, 2001), where change in number of cells of genotype  $i$  in a fixed time interval  $\Delta t$  is Poisson distributed with mean  $v_i \Delta t$ . If the change in number of cells is negative and larger then the subpopulation size then the subpopulation size is updated to be zero.

**Bootstrapping** We use bootstrap resampling method in order to compute confidence intervals for the mean threshold tumor sizes and mean times by resampling 100 times with replacement from the data set obtained from simulations. We then compute the interval which contain 95% of the means of each resampled set.

**Parameterization.** To parametrize the model we assume that the cells under consideration are melanoma cells and rely on (Rew and Wilson, 2000) and (Bozic et al., 2013) for the division and death rates, respectively. Rew and Wilson (2000) report in vivo measurements of the potential doubling times (which is the time which the tumor cells would take to double in number if cell loss was not present) for a large set of cancer types. The division rate is obtained as  $\lambda = \log 2 / T \approx 0.1 \text{ days}^{-1}$ . We select this to be the division rate for wildtype and mutant cells.

Bozic et al. (2013) report the growth rate  $\Delta_w$  for the wildtype melanoma cancer cells from which they deduce the death rate  $\mu_w$  to in the interval  $[0.11, 0.17]$  and we choose  $\mu_w = 0.14 \text{ days}^{-1}$ . Additionally, they observe the growth rate of cancer cells prior to treatment to be 0.01 which we select as the growth rate of mutant cells as we assume that the mutation makes the cancer cells immune to the chemotherapeutic agent. As a result, we choose  $\mu_m = 0.1 - 0.01 = 0.09 \text{ days}^{-1}$  as the death rate for mutant cells.

Aneuploid death rate  $\mu_a$  is set to the same value as the mutant death rates,  $\mu_m = 0.09 \text{ days}^{-1}$ , given that aneuploidy increases resistance to chemotherapeutics, such as cisplatin, by antagonizing cell division (Replogle et al., 2020). Aneuploid birth rate is selected such that the aneuploid growth rate  $\Delta_w \ll \Delta_a \ll \Delta_m$  which means that  $\lambda_a$  belong to the interval  $[0.06, 0.1]$ . For most of the paper we will use  $\lambda_a = 0.0899 \text{ days}^{-1}$  such that aneuploidy can only act as a *stepping stone* for the generation of the mutant which rescues the cancer cell population.

We set the mutation rate  $v$  to be equal to  $10^{-7}$  per gene per cell division (Loeb, 2001) and since we assume that a single target gene confers immunity to chemotherapy we select  $v = 10^{-7}$  per cell division. The missegregation rate is chosen from Bakker et al. (2023) who determined *in silico* that it

must be in the interval  $10^{-3} - 10^{-2}$  per chromosome per cell division. Given that only about one to two chromosome additions are “beneficial” for cancer resistance (see details next paragraph) we choose  $u = 10^{-2}$  per cell division. For the missegregation rate in the drug free environment  $\tilde{u}$  we choose the lower-end value of  $u$  (i.e.  $\tilde{u} = 10^{-3}$  per cell division) as the chemotherapeutic drugs we want to model increase the rate of aneuploidy (Mason et al., 2017, Wang et al., 2019).

The fitness cost  $s$  of aneuploidy before the onset of therapy is difficult to estimate as we are interested in a specific type of aneuploidy which improved the fitness of cancer cells in an environment altered by chemotherapeutic drugs. We derive  $s$  by using the formula  $s = \tilde{u}\lambda_w/f$  and obtaining the fraction of aneuploid cancer cells  $f$  from (Lukow et al., 2021) who mixed together wildtype and aneuploid A375 melanoma cells at 50 : 50 ratio, cultured them in drug-free environment and observed the ratio evolve as a function of time with the aneuploid cells declining to 15% after 24 days. Ippolito et al. (2021) observed that trisomy 2 and 6 are most likely to confer increased resistance against the chemotherapeutic agent vemurafenib for A375 cells. We assume that if a tumor is aneuploid then it most likely has trisomy (Gisselsson et al., 2010) in the pre-treatment environment and that cells with more than one trisomy are very unlikely to survive. Additionally, we assume that all trisomies are equally likely and, as a result, we obtain the percentage of cancer cells with favorable aneuploidy as  $2/22 \times 0.15 \approx 0.0136$  (i.e. 1.36% of pre-treatment cancer cells have the “beneficial” aneuploidy) which we select as the value for  $f$  (this gives us a fitness cost of  $s = 7.3 \times 10^{-3} \text{ days}^{-1}$ ). We note that when we refer to wildtype cancer cells we include those cells which have any aneuploidy except trisomy 2 and 6 as those are the aneuploid cells which are hypothesized to have higher fitness in the environment altered by therapeutics such as vemurafenib.

**Density-dependent growth.** In our analysis we assume that lineages produced by cells from the initial population divide and die independently of each other, which may be unrealistic, as cells usually compete for resources. This is a good approximation as we assume that the drug cause the wildtype population to decline rapidly and, as a result, density effect can be neglected. A more realistic model includes competition for limited resources and spatial structure, which may play an important role in the development of cancer (e.g., Martens et al., 2011). To simulate birth and death rates that depend on the number of cells in the population, we transform the rates of division and death to the following:

$$\begin{aligned}\lambda'_w &= \lambda_w, \\ \mu'_w &= \mu_w, \\ \lambda'_a &= \lambda_a, \\ \mu'_a &= \mu_a + \lambda_a \frac{w + a + m}{K}, \\ \lambda'_m &= \lambda_m, \\ \mu'_m &= \mu_m + \lambda_m \frac{w + a + m}{K}.\end{aligned}$$

where  $K$  is the maximum carrying capacity. The effective carrying capacity of this model is  $K_e = K\Delta_a/\lambda_a \approx 10^6$  for  $K = 10^8$ ,  $\lambda_a = 0.0901$ ,  $\mu_a = 0.09$ , where we define the effective carrying capacity to be the population size at which the aneuploid division rate is equal to the aneuploid death rate.

## Code and data availability.

All source code is available online at <https://github.com/yoavram-lab/EvolutionaryRescue>.

## Results

### Evolutionary rescue probability

In our model, *evolutionary rescue* occurs when resistant cells appear and fixate ( $m_t \gg 1$ ) in the population before the population becomes extinct ( $w_t = a_t = m_t = 0$ ). Aneuploidy may contribute to evolutionary rescue by either preventing (when  $\Delta_a > 0$ ) or delaying (when  $0 > \Delta_a > \Delta_w$ ) the extinction of the population before mutant cells appear and fixate. We assume independence between clonal lineages starting from an initial population of  $N$  wildtype cells (we check the effect of density-dependent growth on our results below). We therefore define  $p_w$  as the probability that a lineage starting from a single wildtype cell avoids extinction by acquiring drug resistance. Thus,  $N^* = 1/p_w$  is the threshold tumor size above which evolutionary rescue is very likely, and the rescue probability is given by

$$p_{\text{rescue}} = 1 - (1 - p_w)^N \approx 1 - e^{-Np_w} = 1 - e^{-N/N^*}. \quad (2)$$

where the approximation  $(1 - p_w) \approx e^{-p_w}$  assumes that  $p_w$  (but not necessarily  $Np_w$ ) is small. Indeed, when  $N < 1/p_w$ , then the probability for evolutionary rescue is  $p_{\text{rescue}} \approx Np_w$  and when  $N > 1/p_w$ , it is  $p_{\text{rescue}} \approx 1$ , justifying the definition of  $N^*$  as the threshold tumor size.

In Appendix A, we use the theory of multi-type branching processes to find approximate expressions eqs. (13), (16) and (20) for  $p_w$  in different regimes. Substituting these into  $N^* = 1/p_w$ , we find approximations for the threshold tumor size,  $N^*$ . For these approximations, an important quantity is  $T^* = (4v\lambda_a^2\Delta_m/\lambda_m)^{-1/2}$ , which is the critical time an aneuploid lineage needs to survive to produce a resistant mutant that avoids random extinction. First, if aneuploidy is very rare ( $u\lambda_a T^* < 1$ ), or if aneuploidy is rare ( $u\lambda_a < -\Delta_a$ ) and very sensitive to the drug ( $\Delta_a T^* < -1$ ), then rescue will likely occur by a direct resistance mutation in a sensitive cell, such that

$$N_m^* \approx \frac{|\Delta_w|}{v\lambda_w} \cdot \frac{\lambda_m}{\Delta_m}. \quad (3)$$

Here,  $|\Delta_w|/(v\lambda_w)$  is the ratio of the rate at which wild-type cells are decreasing in number and the rate at which they are mutating.

Otherwise, aneuploidy is frequent enough ( $u\lambda_a > \max(-\Delta_a, 1/T^*)$ ) to affect the evolution of drug resistance. The threshold tumor size,  $N^*$ , can then be approximated by one of the following cases, depending on  $\Delta_a T^*$ , the change in the log of the aneuploid population size during the critical time,

$$N_a^* \approx \frac{|\Delta_w|}{u\lambda_w} \cdot \begin{cases} \frac{|\Delta_a|}{v\lambda_a} \cdot \frac{\lambda_m}{\Delta_m}, & \Delta_a T^* \ll -1 \text{ (tolerant aneuploids),} \\ 2\lambda_a T^*, & -1 \ll \Delta_a T^* \ll 1 \text{ (stationary aneuploids),} \\ \frac{\lambda_a}{\Delta_a}, & \Delta_a T^* \gg 1 \text{ (resistant aneuploids).} \end{cases} \quad (4)$$

The first line describes the case in which aneuploids are still effectively killed by the treatment, but not as quickly as the wild type. In the second case, the aneuploids are sufficiently resistant that the size of each aneuploid lineage is expected to remain roughly constant. In both of these first two cases, aneuploidy increases the probability of rescue by slowing or halting the decrease of the cancer population, allowing more opportunities for producing resistant mutants. In the third case, aneuploidy provides sufficient resistance for the aneuploid population to re-grow the tumor even without additional resistance mutations. Note that in this case there is no dependence on the parameters characterizing mutants or their production ( $v$ ,  $\lambda_m$ , and  $\Delta_m$ ). Comparing these approximations to results of stochastic evolutionary simulations, we find that the approximations perform very well (Figures 3 and 4). Increasing the the missegregation rate  $u$  and aneuploid growth rate  $\Delta_a$  reduces the threshold tumor size and facilitates the evolution of drug resistance (Figure 4).

Using eqs. (3) and (4), we can find the ratio of threshold tumor size for rescue via aneuploidy ( $u$  is high) or via direct mutation ( $u$  is low),

$$\frac{N_a^*}{N_m^*} \approx \begin{cases} \frac{|\Delta_a|}{u\lambda_a}, & \Delta_a T^* \ll -1, \\ \frac{1}{u} \left( v \cdot \frac{\Delta_m}{\lambda_m} \right)^{1/2}, & -1 \ll \Delta_a T^* \ll 1, \\ v \frac{\Delta_m}{\lambda_m} \cdot \left( u \frac{\Delta_a}{\lambda_a} \right)^{-1}, & \Delta_a T^* \gg 1. \end{cases} \quad (5)$$

In all cases, the effect of aneuploidy increases (i.e., the threshold size ratio decreases) when the aneuploidy rate  $u$  increases (Figure 4B). Increasing the aneuploid growth rate  $\Delta_a$  also leads to an increased role of aneuploidy, although the effect is minor when  $|\Delta_a|$  is small compared to  $T^*$  (Figure 4A). Increasing the mutation rate  $v$  decreases the effect of aneuploidy and increases the probability of evolutionary rescue.

In the first case,  $|\Delta_a|/(u\lambda_a)$  is the ratio of the expected time for an aneuploid lineage to appear,  $1/(u\lambda_a)$ , and the expected time until that lineage disappears,  $1/|\Delta_a|$ . In the third case,  $\left(v \frac{\Delta_m}{\lambda_m}\right) / \left(u \frac{\Delta_a}{\lambda_a}\right)$  is the ratio of the rates of formation of resistant mutants that avoid extinction and partially resistant aneuploids that avoid extinction. In the second case,  $\frac{1}{u} \left( v \cdot \frac{\Delta_m}{\lambda_m} \right)^{1/2} = \sqrt{\frac{\Delta_a}{u\lambda_a} \cdot v \frac{\Delta_m}{\lambda_m} \cdot \left( u \frac{\Delta_a}{\lambda_a} \right)^{-1}}$ , which is the geometric mean of the first and third cases.

Interestingly, increasing both the aneuploid division rate,  $\lambda_a$ , and the aneuploid death rate,  $\mu_a$ , such that the growth rate  $\Delta_a$  remains constant, leads to decreases in  $T^*$ , and therefore to the second case. In this case, increasing the division rate  $\lambda_a$  should also increase the mutation rate  $v\lambda_a$  in aneuploid cells, as mutations mostly occur during division, so overall the threshold tumor size  $N_a^*$  is unaffected by the division rate  $\lambda_a$  (i.e.,  $d\lambda_a T^*/d\lambda_a = 0$ ). Thus, if aneuploids rapidly die due to the drug but compensate by rapidly dividing, further increasing the division rate will *not* facilitate adaptation. This is consistent with experimental findings where aneuploidy confers resistance by decreasing the division rate (Replogle et al., 2020). For the parameter values of  $\lambda_w = 0.1, \lambda_a = 0.0899, \lambda_m = 0.1, \mu_w = 0.14, \mu_a = 0.09, \mu_m = 0.09, u = 10^{-2}, v = 10^{-7}$  we are in the partially resistant aneuploid case and obtain the ratio  $N_a^*/N_m^* \approx |\Delta_a|/u\lambda_a = 0.11$  which means that the presence of aneuploidy reduces the threshold population by approximately 90%. We note that for this parameter regime we have  $N_a^* \approx 4.4 \times 10^6$  and  $N_m^* \approx 4 \times 10^7$  and this allows us to define the following categories: small tumors have size  $N < N_a^*$ , intermediate sized tumors have  $N_a^* < N < N_m^*$  and large tumors have size  $N > N_m^*$ . For the remaining of this paper we use these definitions when referring to small, intermediate or large tumors. Interestingly, the threshold between small and intermediate tumors is similar to the detection threshold of  $4.19 \times 10^6$  for a wide variety of tumors as reported by Avanzini and Antal (2019).

**Density-dependent growth.** In our analysis we used branching processes, which assume that growth (division and death) is density-independent. However, growth may be limited by resources (oxygen, nutrients, etc.) and therefore depend on cell density. We therefore performed stochastic simulations of a logistic growth model with carrying capacity  $K$  (see Methods). We find that our approximations agree with results of simulations with density-dependent growth for biologically relevant parameter values (Figure 8).

**Standing vs. de-novo genetic variation.** In the above we assumed that at the onset of drug treatment, the initial tumor consisted entirely of wildtype cells that are drug sensitive. However, aneuploid cells are likely generated even before onset of treatment at some rate  $\tilde{u} \leq u$  (because the treatment itself may promote generation of aneuploid cells (Mason et al., 2017, Wang et al., 2019)), which are likely to have a deleterious effect in the absence of the drug,  $s$  (Giam and Rancati, 2015, Replogle et al.,

2020). But if the number of cells in the tumor  $N$  is large (as expected if the tumor is to be treated with a drug), there may already be a fraction  $f \approx \tilde{u}\lambda_w/s$  (we assume that the division rate of the wildtype in a drug-free environment is equal to the division rate of the wildtype in the environment affected by the anti-cancer drug) of aneuploid cells in the population.

Therefore, the threshold tumor size with standing generation variation,  $\tilde{N}_a^*$ , is similar to the ratio with de-novo variation,  $N_a^*$ , except that the sensitive growth rate  $|\Delta_w|$  is replaced with the aneuploidy cost,  $s$ , such that

$$\frac{\tilde{N}_a^*}{N_a^*} = \frac{u}{\tilde{u}} \frac{s}{|\Delta_w|}. \quad (6)$$

Therefore, standing genetic variation will drive adaptation to the drug if  $\Delta_w$  is very negative due to a stronger effect of the drug on sensitive cells, or if  $s$  is very small due to a low cost of aneuploidy in the pre-drug conditions. In contrast, de-novo aneuploids will have a stronger effect on adaptation if the aneuploidy cost  $s$  is large, the effect of the drug is weak ( $\Delta_w$  is small), or if the drug induces the appearance of aneuploid cells ( $u > \tilde{u}$ ). Comparing these approximations to results of stochastic evolutionary simulations, we find that the approximations perform very well (Figure 5).

For the parameter values of  $\lambda_w = 0.1$ ,  $\mu_w = 0.14$ ,  $u = 10^{-2}$ ,  $\tilde{u} = 10^{-3}$ ,  $s = 7.3 \cdot 10^{-3}$  the ratio of the threshold population sizes is  $\tilde{N}_a^*/N_a^* \approx 1.825$  which means that de-novo genetic variation is the main driver of adaptation.

Using eqs. (3), (4) and (6), we can find the ratio of threshold tumor size for rescue via standing genetic variation to the threshold for direct mutation,

$$\frac{\tilde{N}_a^*}{N_m^*} = \frac{\tilde{N}_a^*}{N_a^*} \times \frac{N_a^*}{N_m^*} \approx \frac{s}{|\Delta_w|} \begin{cases} \frac{|\Delta_a|}{\tilde{u}\lambda_a}, & \Delta_a T^* \ll -1, \\ \frac{1}{\tilde{u}} \left( v \cdot \frac{\Delta_m}{\lambda_m} \right)^{1/2}, & -1 \ll \Delta_a T^* \ll 1, \\ v \frac{\Delta_m}{\lambda_m} \cdot \left( \tilde{u} \frac{\Delta_a}{\lambda_a} \right)^{-1}, & \Delta_a T^* \gg 1. \end{cases} \quad (7)$$

We observe that evolutionary rescue through direct mutation is more likely if the cost of aneuploidy  $s$  is very large or the effect of the drug  $\Delta_w$  is small. In contrast, standing genetic variation will drive adaptation if the pre-treatment chromosome missegregation rate  $\tilde{u}$  is very large. The ratio does not depend on the rate of chromosome missegregation induced by the drug  $u$ . However, if the growth rate of aneuploidy  $\Delta_a$  increases then evolutionary rescue is driven by standing genetic variation. For the parameter values of  $\lambda_w = 0.1$ ,  $\lambda_a = 0.0899$ ,  $\lambda_m = 0.1$ ,  $\mu_w = 0.14$ ,  $\mu_a = 0.09$ ,  $\mu_m = 0.09$ ,  $\tilde{u} = 10^{-3}$ ,  $v = 10^{-7}$  we are in the partially resistant aneuploid case and obtain the ratio  $\tilde{N}_a^*/N_m^* \approx \frac{s}{|\Delta_w|} \times \frac{|\Delta_a|}{\tilde{u}\lambda_a} = 0.356$  which means that standing genetic variation reduces the threshold population by approximately 65%. We observe that while standing genetic variation does not drive emergence of drug resistance when compared to de-novo aneuploids it does offer an advantage when compared with direct mutation.

## Recurrence time due to evolutionary rescue

Even when evolutionary rescue occurs and leads to recurrence of the tumor, it may take a long time. When the expected number of resistant lineages that avoid extinction is small the overall expected recurrence time can be estimated by adding two terms: the mean waiting time for evolutionary rescue—the appearance of a resistant lineage that avoid extinction (which we denote the mean evolutionary rescue time) and the expected time for proliferation of that lineage back to the original tumor size,  $N$  (which we denote the mean proliferation time). However, when the expected number of resistant lineages is large the population of mutant cells behaves deterministically and the mean recurrence time cannot be separated into the mean evolutionary rescue time and mean proliferation time. Of particular interest is the distribution of the evolutionary rescue time and recurrence time in the parameter regime  $\Delta_a T^* \ll 1$  (partially tolerant aneuploids) for which we select  $\lambda_w = 0.1$ ,  $\lambda_a = 0.0899$ ,  $\lambda_m = 0.1$ ,  $\mu_w = 0.14$ ,  $\mu_a = 0.09$ ,  $\mu_m = 0.09$ ,  $u = 10^{-2}$ ,  $v = 10^{-7}$ .



**Evolutionary rescue time.** In Appendix C we derive an approximation for  $\tau_m$ , the expected evolutionary rescue time without aneuploidy ( $u = 0$ ), and  $\tau_a$ , the expected rescue time with aneuploidy ( $u > 0$ ). Figures 9 and 13 shows the agreement between these approximations and simulation results for small, intermediate and large tumor sizes. Additionally, we note that  $\tau_a$  has the following asymptotic behaviour:

$$\tau_a \approx \begin{cases} \frac{1}{|\Delta_w|} + \frac{1}{|\Delta_a|}, & N \ll N_a^*, \\ (v\lambda_w N p_m)^{-1}, & N \gg N_m^*. \end{cases} \quad (8)$$

Interestingly, for small tumors the mean evolutionary rescue time is a function of the wildtype and aneuploid growth rates and independent of all of other model parameters including tumor size  $N$  (Figure 13). Increasing either the wildtype or aneuploid growth rates lead to an increase in the mean time. This can be interpreted that by increasing either growth rates the wildtype or aneuploid cells will last longer and will be able to produce a rescue mutation at latter times. Using the parameters that we have selected we observe that  $|\Delta_w|^{-1} = 0.04$  and  $|\Delta_a|^{-1} = 10^{-4}$  such that the mean evolutionary rescue time is determined by the aneuploid growth rate, i.e.  $\tau_a \approx 1/|\Delta_a|$ . For large tumors, we observe that the evolutionary rescue time is exponentially distributed with rate  $v\lambda_w N p_m$  which is independent of parameters characterizing aneuploids or their production ( $u$ ,  $\lambda_a$ , and  $\Delta_a$ ). Increasing the mutation rate per mitosis  $v\lambda_w$  leads to a faster appearance of a rescue mutation. Note that in the second case increasing the tumor size leads to smaller mean evolutionary rescue time as the wildtype is able to produce a rescue lineage faster.

When a fraction  $f \approx 1.36\%$  of the initial cancer cell population is aneuploid we calculate the mean evolutionary rescue time in Equation (31) which we plot in Figure 16. We note that standing genetic variation reduces the mean evolutionary rescue time only for intermediary sized tumors but not for large or small tumors.

**Recurrence time.** In Appendix D we approximate the mean time for the population of mutant cancer cells to reach the initial population size  $N$  which we denote as the recurrence time. Figure 7 shows the agreement between our approximations and simulations. For values of  $N$  smaller then  $10^8$  the mean recurrence time can be approximated as the sum of the mean time for the first rescue mutation to appear and the mean time for the lineage generated by that mutation to reach size  $N$ . For  $N > 10^8$  the behavior of the mutant cancer cell population is deterministic and the mean recurrence time becomes constant. We note that  $\tau_a^r$  has the following asymptotic behavior:

$$\tau_a^r \approx \begin{cases} \frac{1}{|\Delta_w|} + \frac{1}{|\Delta_a|} + \frac{\log p_m N}{\Delta_m}, & N \ll N_a^*, \\ \frac{1}{\Delta_m} \log \frac{\Delta_m - \Delta_w}{v\lambda_w}, & N \gg N_m^*. \end{cases} \quad (9)$$

In the first case, when tumor is small, the mean recurrence time grows logarithmically with tumor size  $N$  and is the same order of magnitude as the mean evolutionary rescue time (Figure 14). Increasing the mutant growth rate  $\Delta_m$  leads to shorter recurrence times while increasing the wildtype and aneuploid growth rates  $\Delta_w$  and  $\Delta_a$ , retrospectively, increases the recurrence time. In the second case, when tumor is large, we observe that increasing either the mutant growth rare  $\Delta_m$  or the mutation rate  $v$  leads to a decrease in the time needed for the tumor to rebound to its initial size. Additionally, drugs which significantly increase the wildtype death rate  $\mu_w$  and do not affect the division rate  $\lambda_w$  delays cancer relapse. Consequently, patients which take such drugs require a longer period of monitoring to guarantee the effectiveness of the treatment.

**Distribution of evolutionary rescue time with and without aneuploidy.** In Appendix E we derive the probability that by time  $t$  a successful mutant has been generated. Figure 6A show the agreement between our formula and simulation results for the case when aneuploidy is present and when it is absent. We observe that aneuploidy start to have an effect on adaptation for timescales greater then 100 days.

**Distribution of recurrence time.** In Appendix F we derive the probability that mutant cancer cell population reaches  $N$  at time  $t$ . Figure 6B shows agreement between our approximations and stochastic simulations for various values of  $N$ . Additionally, we derived the distribution of the recurrence time and plotted our result in Figure 11 alongside simulations for the case  $N = 10^6$  (small tumor) and we note that the distribution is wide and rights-skewed. It is highly unlikely to observe the recurrence of tumors at times smaller then  $\frac{1}{\Delta_m} \log \frac{\Delta_m - \Delta_w}{v\lambda_w} \approx 1542$  days for the parameter values  $\lambda_w = 0.1, \lambda_a = 0.0899, \lambda_m = 0.1, \mu_w = 0.14, \mu_a = 0.09, \mu_m = 0.09, u = 10^{-2}, v = 10^{-7}$  and independent of initial tumor size  $N$  (Figure 6B).

The recurrence can also be defined as the time necessary for the tumor size to reach a detection threshold  $M$ . We derive the mean recurrence time to detection size  $M = 10^7$  in Appendix D and plot in Figure 15 with simulations. We observe that for small and intermediate sized tumors the effect of the detection size is negligible when compared to  $\tau_a'$ . However, for large tumors the mean recurrence time to detection size  $M$  decreases logarithmically with tumor size  $N$ .

Most clinical trials report data on the distribution of recurrence time measured from a varying time of surgery (Avanzini and Antal, 2019) with chemotherapy usually following after. Therefore, since only undetected secondary tumors are present at the time of the administration of the anti-cancer drug we lack knowledge of the size of the tumors and we cannot compare the empirical distributions to our predictions. However, we expect that the variability of secondary tumors to average out across large cohorts of patients and, as a result, we can use the mean recurrence time.

## Discussion

We have modeled a tumor—a population of cancer cells—exposed to drug treatment that causes the population to decline in size towards potential extinction. In this scenario, the tumor can be "evolutionary rescued", or escape extinction, via two paths. In the direct path, a sensitive cell acquires a mutation that confers resistance that allows it to rapidly grow. In the indirect path, a sensitive cell first becomes aneuploid, which diminishes the effect of the drug, and then an aneuploid cell acquires a mutation that confers resistance (Figure 1).

Using multitype branching processes, we derived the probability of evolutionary rescue of the population of cancer cells under different scenarios for the effect of aneuploidy, ranging from tolerance to partial resistance. We obtained exact and approximate expressions for the probability of evolutionary rescue (eq. (2)). Our results show that the probability of evolutionary rescue increases with the initial tumor size  $N$ , the sensitive growth rate  $\Delta_w$ , the mutation rate  $v$ , and the aneuploidy rate  $u$ .

**Evolutionary rescue** When aneuploid cells are partially resistant to the drug ( $\Delta_w \ll 0 \ll \Delta_a \ll \Delta_m$ ), evolutionary rescue can be approximated by a one-step process in which aneuploidy itself rescues the population (Figure 4A). When aneuploidy only provides tolerance to the drug ( $\Delta_w \ll \Delta_a \ll 0 \ll \Delta_m$ ), it cannot rescue the population. Instead, it acts as a *stepping stone* through which the resistant mutant can appear more rapidly, given that the aneuploid cell population declines slower then the sensitive cell population (Figure 2). In this case, aneuploidy provides two benefits. First, it delays the extinction of the population—providing more time for appearance of the resistance mutation. Second, it increases the population size relative to a sensitive population—providing more cells in which mutations can occur, i.e., it increases the mutation supply,  $Nuv\lambda_w\lambda_a/|\Delta_w\Delta_a|$ .

We find that aneuploidy can have a significant effect on evolutionary rescue as it reduces the threshold population size by at least one order of magnitude even when aneuploidy is tolerant (Figure 3). Interestingly, aneuploidy is unlikely to contribute to evolutionary rescue in primary tumors in which the number of cells is large enough ( $N \gg N_m^* \approx 4 \times 10^7$ ) for the appearance of resistant mutation directly in sensitive cells before these cells become extinct (Figure 3). However, aneuploidy can have a crucial role in evolutionary rescue of secondary tumors, in which the number of sensitive cells may be

below the detection threshold of  $\sim 10^7$  (Bozic et al., 2013). This can have an impact on the recurrence of cancer after the resection of the primary tumor through secondary tumors which are too small to be detected and for which chemotherapy is employed to prevent cancer relapse and are estimated to cause the majority of cancer-related deaths (Chaffer and Weinberg, 2011). This is reinforced by the fact that metastases have been shown to have higher chromosome missegregation rate two to three orders of magnitude higher than primary tumors (Kimmel et al., 2023).

Given the fact that the mean time for such secondary tumors to overcome chemotherapy can be of the order of 1000 days (Figure 9A), this can explain the reappearance of cancer even after initial remission. The theoretical predictions for the mean rescue time for tumors smaller than  $10^8$  is greater than 4 years which is consistent with previous estimates of the recurrence time of tumors after resection (Avanzini and Antal, 2019).

We hypothesized that presence of *standing variation*—the existence of a subpopulation of aneuploid cancer cells before therapy begins—can facilitate evolutionary rescue by reducing the waiting time for the appearance of aneuploid cells. However, we observe that for reasonable parameter values evolutionary rescue is more likely to occur through de-novo aneuploidy (Figure 5). If the fraction of the tumor cells which have the “beneficial” aneuploidy is  $f \gg \frac{u\lambda_w}{|\Delta_w|} \approx 2.5\%$  then evolutionary rescue is more likely to occur through this existing standing variation, rather than through *de novo* aneuploid cells. In that case, evolutionary rescue occurs through a single step by the aneuploid cells acquiring a beneficial mutation and the probability of evolutionary rescue is given by  $1 - \exp(-N/\tilde{N}_a^*)$  (Figure 12).

**Experimental future direction** Our model’s predictions may be tested by experiments (Martin et al., 2013). For example, to study the effects of initial tumor size on the probability of evolutionary rescue, a large culture mass can be propagated from a single cancer cell in permissive conditions and then diluted to a range of starting tumor sizes. Afterwards, these tumors may be exposed to anti-cancer drugs that induces aneuploidy or to saline solution for control (Ippolito et al., 2021). Cell density can then be measured by optical density and a population exposed to the drug is considered extinct if the optical density is lower when compared to the control case with no cells present. We compare to the predictions of our model to see if the tumors with initial size below the threshold (4) are more likely to go extinct.

Additionally, we can test our model’s predictions with data from patients. Given the type of cancer they have and the degree of “beneficial” aneuploidy, we can obtain the parameters for our model and predict with what probability will the cancer relapse after treatment.

**Directions of future research** Even though our model has been designed for cancer it can be extended to understand evolutionary rescue in different biological contexts, for example, how yeast subject to stress can overcome extinction with the help of aneuploidy (Pompei and Cosentino Lagomarsino, 2023). Additionally, the heterogeneity of aneuploidy is a fact we did not account for, as not all the aneuploidy lineages generated have the same growth rate  $\Delta_a$ . This can be corrected by fixing the aneuploidy death rates and sampling the aneuploidy growth rates from a distribution  $f(\Delta_a|\mu_a)$  Martin et al. (2013). Furthermore, tumor heterogeneity is also a factor for pre-existing genetic variation where the fitness of the aneuploid cells can be drawn from a distribution upon which selection acts when the tumor is exposed to a strong stress.

We have assumed that cancer cell lineages are independent of each other. However, this may not be the case, as cancer cells compete for resources (e.g., blood supply). Nevertheless, we find that when the effective carrying capacity is not too large ( $K \sim 10^8, K_e \sim 10^6$ ) our approximation for the probability of evolutionary rescue agrees with results of stochastic simulations with density-dependent growth (Figure 8). Future work may focus on scenarios with small carrying capacity by analyzing density-dependent branching processes (Harris, 1963, Klebaner, 1997).

Solid tumors are spatially heterogeneous with different genotypes inhabiting cellular niches and immune infiltration impacting growth in affected regions (Galon et al., 2010, Varrone et al., 2023). This has the potential to impact the probability of overcoming chemotherapy (Martens et al., 2011). Future work should take into consideration the spatial structure of the tumor and its effect on the probability of evolutionary rescue.

An additional limitation of our model is the choice of parameters which are based on a specific set of assumptions which might not be true for many tumor. As a result, incorporating a wider distribution of parameters would be a beneficial extension for our model.

**Conclusions** Our paper analyzed the role that aneuploidy plays in tumor adaptation to the effects of anti-cancer drugs. Our study quantitatively confirms that aneuploidy plays an important role in tumors overcoming exposure to chemotherapeutic drugs when the tumor size is small or intermediate. Very large tumors can escape anti-cancer drugs through direct mutation while smaller ones are able to obtain the beneficial mutation through an aneuploid intermediary (Figure 3). As a result, therapies which increase the rate of aneuploidy in tumors in order to combat cancer might have an adverse effect on patient outcomes.

## Acknowledgements

We thank Hildegard Uecker for discussions and comments. This work was supported in part by the Israel Science Foundation (ISF 552/19, YR), the US–Israel Binational Science Foundation (BSF 2021276, YR), Minerva Stiftung Center for Lab Evolution (YR), Ela Kodesz Institute for Research on Cancer Development and Prevention (RS), the Simons Foundation (Investigator in Mathematical Modeling of Living Systems #508600, DBW), the Sloan Foundation Research Fellowship (FG-2021-16667, DBW), the NSF grant (#2146260, DBW), [Uri Ben-David acknowledgements](#)

## References

- Allen, L. J. (2010), *An introduction to stochastic processes with applications to biology*, CRC press.
- Avanzini, S. and Antal, T. (2019), ‘Cancer recurrence times from a branching process model’, *PLoS computational biology* **15**(11), e1007423.
- Bakker, B., Schubert, M., Bolhaqueiro, A. C., Kops, G. J., Spierings, D. C. and Foijer, F. (2023), ‘Predicting CIN rates from single-cell whole genome sequencing data using an *in silico* model’, *bioRxiv* pp. 2023–02.
- Barton, G. (1989), *Elements of Green’s functions and propagation: potentials, diffusion, and waves*, Oxford University Press.
- Ben-David, U. and Amon, A. (2020), ‘Context is everything: aneuploidy in cancer’, *Nature Reviews Genetics* **21**(1), 44–62.
- Bozic, I., Reiter, J. G., Allen, B., Antal, T., Chatterjee, K., Shah, P., Moon, Y. S., Yaquibie, A., Kelly, N., Le, D. T. et al. (2013), ‘Evolutionary dynamics of cancer in response to targeted combination therapy’, *eLife* **2**, e00747.
- Brauner, A., Fridman, O., Gefen, O. and Balaban, N. Q. (2016), ‘Distinguishing between resistance, tolerance and persistence to antibiotic treatment’, *Nature Reviews Microbiology* **14**(5), 320–330.
- Carja, O. and Plotkin, J. B. (2017), ‘The evolutionary advantage of heritable phenotypic heterogeneity’, *Scientific reports* **7**(1), 1–12.

- Carja, O. and Plotkin, J. B. (2019), ‘Evolutionary rescue through partly heritable phenotypic variability’, *Genetics* **211**(3), 977–988.
- Carlson, J. A. (2003), ‘Tumor doubling time of cutaneous melanoma and its metastasis’, *The American journal of dermatopathology* **25**(4), 291–299.
- Chaffer, C. L. and Weinberg, R. A. (2011), ‘A perspective on cancer cell metastasis’, *science* **331**(6024), 1559–1564.
- Cobbold, C. A. and Stana, R. (2020), ‘Should I stay or should I go: partially sedentary populations can outperform fully dispersing populations in response to climate-induced range shifts’, *Bulletin of Mathematical Biology* **82**(2), 1–21.
- Del Monte, U. (2009), ‘Does the cell number  $10^9$  still really fit one gram of tumor tissue?’, *Cell cycle* **8**(3), 505–506.
- Galon, J., Dieu-Nosjean, M., Tartour, E., Sautes-Fridman, C., Fridman, W. et al. (2010), ‘Immune infiltration in human tumors: a prognostic factor that should not be ignored’, *Oncogene* **29**(8), 1093–1102.
- Giam, M. and Rancati, G. (2015), ‘Aneuploidy and chromosomal instability in cancer: a jackpot to chaos’, *Cell division* **10**(1), 1–12.
- Gillespie, D. T. (1976), ‘A general method for numerically simulating the stochastic time evolution of coupled chemical reactions’, *Journal of computational physics* **22**(4), 403–434.
- Gillespie, D. T. (1977), ‘Exact stochastic simulation of coupled chemical reactions’, *The journal of physical chemistry* **81**(25), 2340–2361.
- Gillespie, D. T. (2001), ‘Approximate accelerated stochastic simulation of chemically reacting systems’, *The Journal of chemical physics* **115**(4), 1716–1733.
- Gisselsson, D., Jin, Y., Lindgren, D., Persson, J., Gisselsson, L., Hanks, S., Sehic, D., Mengelbier, L. H., Øra, I., Rahman, N. et al. (2010), ‘Generation of trisomies in cancer cells by multipolar mitosis and incomplete cytokinesis’, *Proceedings of the National Academy of Sciences* **107**(47), 20489–20493.
- Gomulkiewicz, R. and Holt, R. D. (1995), ‘When does evolution by natural selection prevent extinction?’, *Evolution* pp. 201–207.
- Gunnarsson, E. B., De, S., Leder, K. and Foo, J. (2020), ‘Understanding the role of phenotypic switching in cancer drug resistance’, *Journal of theoretical biology* **490**, 110162.
- Harris, T. E. (1963), *The theory of branching processes*, Vol. 6, Springer Berlin.
- Harsch, M. A., Zhou, Y., HilleRisLambers, J. and Kot, M. (2014), ‘Keeping pace with climate change: stage-structured moving-habitat models’, *The American Naturalist* **184**(1), 25–37.
- Ippolito, M. R., Martis, V., Martin, S., Tijhuis, A. E., Hong, C., Wardenaar, R., Dumont, M., Zerbib, J., Spierings, D. C., Fachinetti, D. et al. (2021), ‘Gene copy-number changes and chromosomal instability induced by aneuploidy confer resistance to chemotherapy’, *Developmental cell* **56**(17), 2440–2454.
- Kimmel, G. J., Beck, R. J., Yu, X., Veith, T., Bakhoum, S., Altrock, P. M. and Andor, N. (2023), ‘Intra-tumor heterogeneity, turnover rate and karyotype space shape susceptibility to missegregation-induced extinction’, *PLOS Computational Biology* **19**(1), e1010815.

- Klebaner, F. (1997), Population and density dependent branching processes, in ‘Classical and modern branching processes’, Springer, pp. 165–169.
- Kocarnik, J. M., Compton, K., Dean, F. E., Fu, W., Gaw, B. L., Harvey, J. D., Henrikson, H. J., Lu, D., Pennini, A., Xu, R. et al. (2022), ‘Cancer incidence, mortality, years of life lost, years lived with disability, and disability-adjusted life years for 29 cancer groups from 2010 to 2019: a systematic analysis for the global burden of disease study 2019’, *JAMA oncology* **8**(3), 420–444.
- Lee, H.-S., Lee, N. C., Kouprina, N., Kim, J.-H., Kagansky, A., Bates, S., Trepel, J. B., Pommier, Y., Sackett, D. and Larionov, V. (2016), ‘Effects of anticancer drugs on chromosome instability and new clinical implications for tumor-suppressing therapies’, *Cancer research* **76**(4), 902–911.
- Levien, E., Min, J., Kondev, J. and Amir, A. (2021), ‘Non-genetic variability in microbial populations: survival strategy or nuisance?’, *Reports on Progress in Physics* **84**(11), 116601.
- Loeb, L. A. (2001), ‘A mutator phenotype in cancer’, *Cancer research* **61**(8), 3230–3239.
- Lukow, D. A., Sausville, E. L., Suri, P., Chunduri, N. K., Wieland, A., Leu, J., Smith, J. C., Girish, V., Kumar, A. A., Kendall, J. et al. (2021), ‘Chromosomal instability accelerates the evolution of resistance to anti-cancer therapies’, *Developmental cell* **56**(17), 2427–2439.
- Martens, E. A., Kostadinov, R., Maley, C. C. and Hallatschek, O. (2011), ‘Spatial structure increases the waiting time for cancer’, *New journal of physics* **13**(11), 115014.
- Martin, G., Aguilée, R., Ramsayer, J., Kaltz, O. and Ronce, O. (2013), ‘The probability of evolutionary rescue: towards a quantitative comparison between theory and evolution experiments’, *Philosophical Transactions of the Royal Society B: Biological Sciences* **368**(1610), 20120088.
- Mason, J. M., Wei, X., Fletcher, G. C., Kiarash, R., Brokx, R., Hodgson, R., Beletskaya, I., Bray, M. R. and Mak, T. W. (2017), ‘Functional characterization of cfi-402257, a potent and selective mps1/ttk kinase inhibitor, for the treatment of cancer’, *Proceedings of the National Academy of Sciences* **114**(12), 3127–3132.
- Orr, H. A. and Unckless, R. L. (2008), ‘Population extinction and the genetics of adaptation’, *The American Naturalist* **172**(2), 160–169.
- Orr, H. A. and Unckless, R. L. (2014), ‘The population genetics of evolutionary rescue’, *PLoS genetics* **10**(8), e1004551.
- Pompei, S. and Cosentino Lagomarsino, M. (2023), ‘A fitness trade-off explains the early fate of yeast aneuploids with chromosome gains’, *Proceedings of the National Academy of Sciences* **120**(15), e2211687120.
- Replogle, J. M., Zhou, W., Amaro, A. E., McFarland, J. M., Villalobos-Ortiz, M., Ryan, J., Letai, A., Yilmaz, O., Sheltzer, J., Lippard, S. J. et al. (2020), ‘Aneuploidy increases resistance to chemotherapeutics by antagonizing cell division’, *Proceedings of the National Academy of Sciences* **117**(48), 30566–30576.
- Rew, D. and Wilson, G. (2000), ‘Cell production rates in human tissues and tumours and their significance. part ii: clinical data’, *European Journal of Surgical Oncology (EJSO)* **26**(4), 405–417.
- Rutledge, S. D., Douglas, T. A., Nicholson, J. M., Vila-Casadesús, M., Kantzler, C. L., Wangsa, D., Barroso-Vilares, M., Kale, S. D., Logarinho, E. and Cimini, D. (2016), ‘Selective advantage of trisomic human cells cultured in non-standard conditions’, *Scientific reports* **6**(1), 22828.

- Schukken, K. M. and Fojier, F. (2018), ‘CIN and aneuploidy: different concepts, different consequences’, *Bioessays* **40**(1), 1700147.
- Smith, J. C. and Sheltzer, J. M. (2018), ‘Systematic identification of mutations and copy number alterations associated with cancer patient prognosis’, *elife* **7**, e39217.
- Tanaka, M. M. and Wahl, L. M. (2022), ‘Surviving environmental change: when increasing population size can increase extinction risk’, *Proceedings of the Royal Society B* **289**(1976), 20220439.
- Uecker, H. and Hermisson, J. (2011), ‘On the fixation process of a beneficial mutation in a variable environment’, *Genetics* **188**(4), 915–930.
- Uecker, H. and Hermisson, J. (2016), ‘The role of recombination in evolutionary rescue’, *Genetics* **202**(2), 721–732.
- Uecker, H., Otto, S. P. and Hermisson, J. (2014), ‘Evolutionary rescue in structured populations’, *The American Naturalist* **183**(1), E17–E35.
- Uecker, H., Setter, D. and Hermisson, J. (2015), ‘Adaptive gene introgression after secondary contact’, *Journal of mathematical biology* **70**, 1523–1580.
- Van Rossum, G. and Others (2007), Python programming language, in ‘USENIX Annu. Tech. Conf.’.
- Varrone, M., Tavernari, D., Santamaria-Martínez, A., Walsh, L. A. and Ciriello, G. (2023), ‘Cellcharter reveals spatial cell niches associated with tissue remodeling and cell plasticity’, *Nature Genetics* pp. 1–11.
- Wang, S., Zhang, M., Liang, D., Sun, W., Zhang, C., Jiang, M., Liu, J., Li, J., Li, C., Yang, X. et al. (2019), ‘Molecular design and anticancer activities of small-molecule monopolar spindle 1 inhibitors: A medicinal chemistry perspective’, *European Journal of Medicinal Chemistry* **175**, 247–268.
- Weissman, D. B., Desai, M. M., Fisher, D. S. and Feldman, M. W. (2009), ‘The rate at which asexual populations cross fitness valleys’, *Theoretical population biology* **75**(4), 286–300.
- Weissman, D. B., Feldman, M. W. and Fisher, D. S. (2010), ‘The rate of fitness-valley crossing in sexual populations’, *Genetics* **186**(4), 1389–1410.
- Wilson, B. A., Pennings, P. S. and Petrov, D. A. (2017), ‘Soft selective sweeps in evolutionary rescue’, *Genetics* **205**(4), 1573–1586.
- Zhou, Y. (2022), ‘Range shifts under constant-speed and accelerated climate warming’, *Bulletin of Mathematical Biology* **84**(1), 1.

	Name	Value	Units	References
$N$	Initial tumor size	$10^7 - 10^9$	cells	Del Monte (2009)
$\lambda_w$	Wildtype division rate	0.1	1/days	Bozic et al. (2013), Rew and Wilson (2000)
$\mu_w$	Wildtype death rate	0.11 – 0.17	1/days	Bozic et al. (2013)
$\lambda_a$	Aneuploid division rate*	0.06 – 0.1	1/days	-
$\mu_a$	Aneuploid death rate*	0.09	1/days	-
$\lambda_m$	Mutant division rate	0.1	1/days	Bozic et al. (2013), Rew and Wilson (2000)
$\mu_m$	Mutant death rate	0.09	1/days	Bozic et al. (2013), Carlson (2003)
$u$	Missegregation rate	$10^{-3} - 10^{-2}$	1/cell division	Bakker et al. (2023)
$v$	Mutation rate	$10^{-9} - 10^{-7}$	1/cell division	Bozic et al. (2013), Loeb (2001)
$\tilde{u}$	Missegregation rate in the drug free environment*	$10^{-3}$	1/cell division	-
$s$	Selection coefficient of aneuploidy in the drug free environment	$7.3 \cdot 10^{-3}$	1/days	Lukow et al. (2021)

**Table 1: Model parameters.** We have modified the parameters from Bozic et al. (2013) such that wildtype/mutant division rate is  $\lambda_{w,m} = \log 2/T \approx 0.1$  instead of their value of 0.14 where  $T$  is the doubling time in the absence of cellular death obtained from Rew and Wilson (2000).



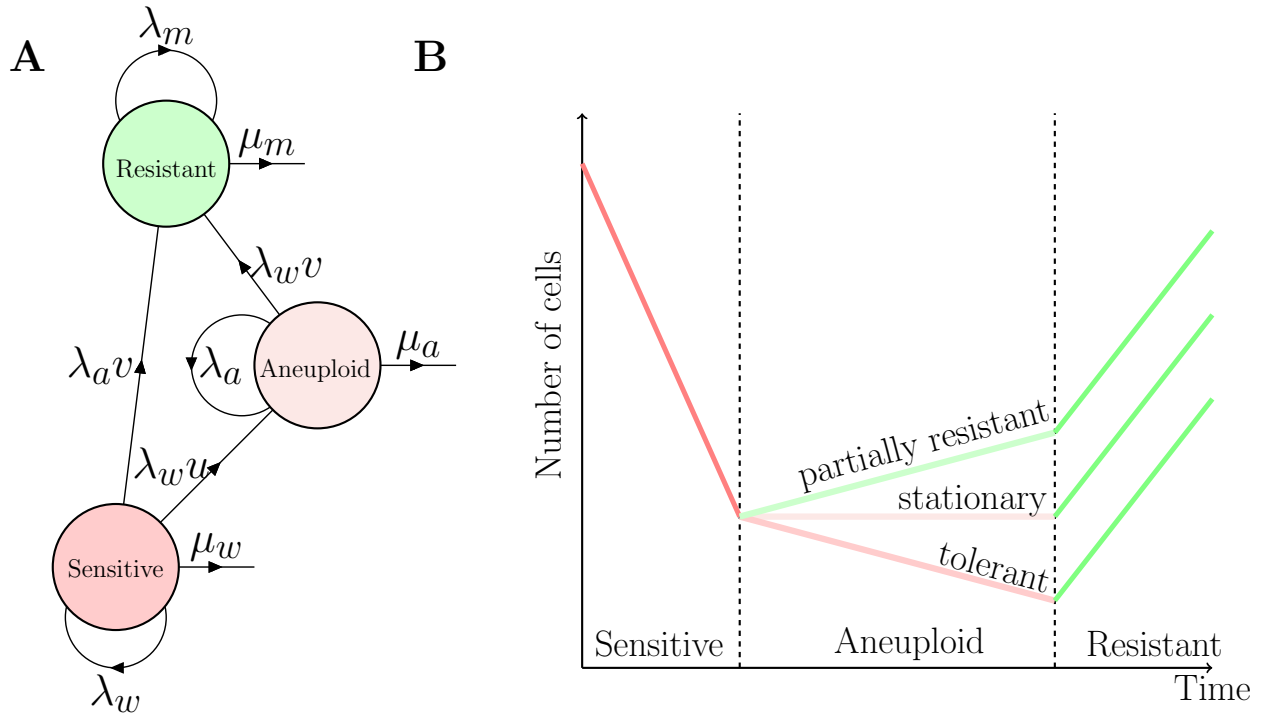


**Figure 1: Model illustration.** (A) A population of cancer cells is composed of wildtype, aneuploid, and mutant cells, which divide with rates  $\lambda_w$ ,  $\lambda_a$ , and  $\lambda_m$  and die at rates  $\mu_w$ ,  $\mu_a$ , and  $\mu_m$ , respectively. Wildtype cells can divide and become aneuploid at rate  $\lambda_w v$ . Both aneuploid and wildtype cells can divide and acquire a beneficial mutation with rate  $v\lambda_a$  and  $v\lambda_w$ , respectively. Color denotes the relative growth rates of the three genotypes such that  $\lambda_w - \mu_w < \lambda_a - \mu_a < \lambda_m - \mu_m$ . (B) The wildtype and the mutant are susceptible and resistant, respectively, to the drug. The aneuploid may be tolerant, stationary and partially resistant.

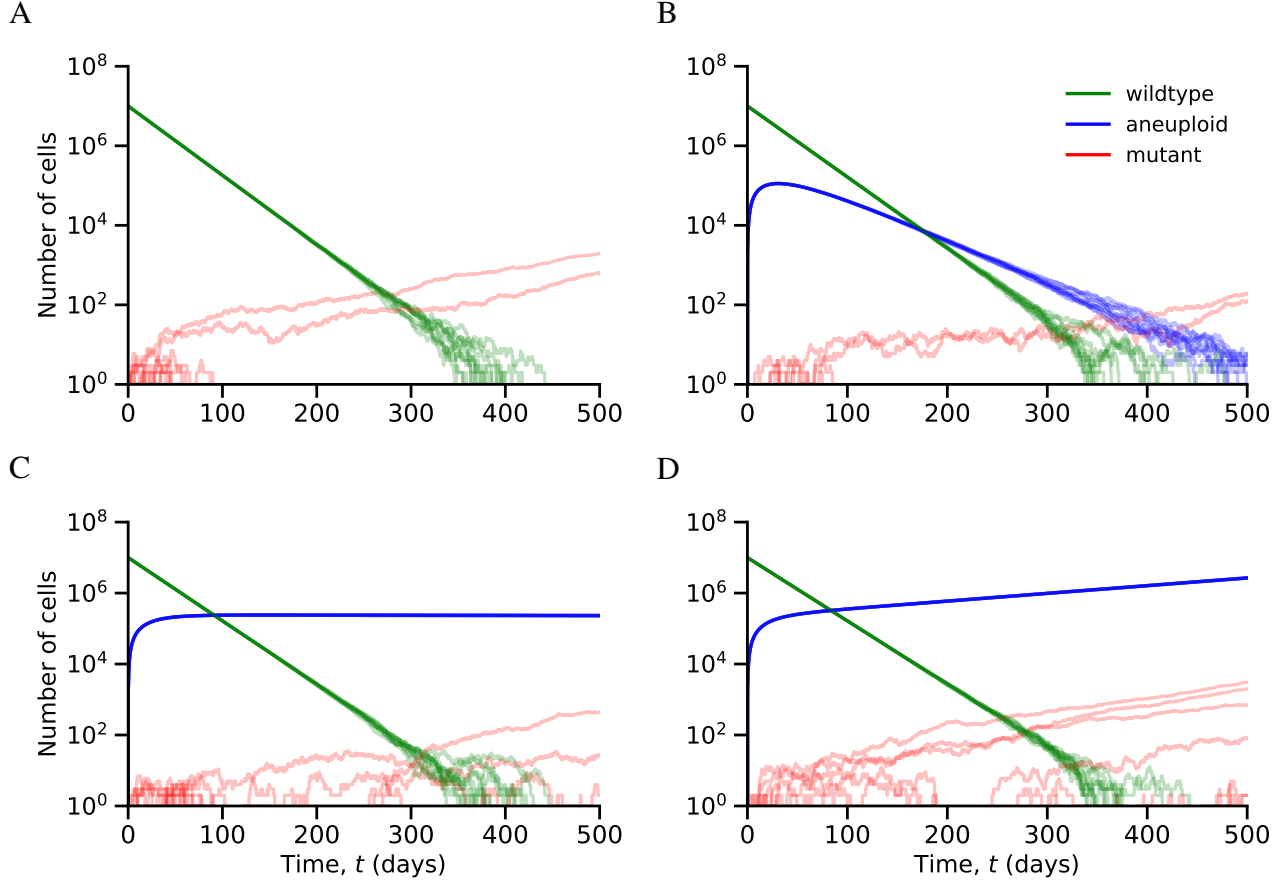


**Figure 2: Sample trajectories of the different genotype frequencies.** (A) When the missegregation rate  $u = 0$  evolutionary rescue is only possible through direct mutation and in most cases the tumor will be killed by the drug. (B) When the aneuploidy growth rate  $\Delta_a \ll 0$  we observe similar dynamic to case (A) as direct mutation is the only viable route toward evolutionary rescue for the tumor. (C) Intermediate aneuploid growth rates  $\Delta_a \approx 0$  leads to the appearance of aneuploid lineages even after the wildtype population has gone extinct thus increasing the chance of evolutionary rescue. (D) As the growth rate of the aneuploid becomes positive we observe that the tumour is rescued by the aneuploid cancer cell population. Each plot features 10 trajectories of  $(w_t, a_t, m_t)$  as a function of time  $t$  for the following parameter values:  $\lambda_w = 0.1, \lambda_m = 0.1, \mu_w = 0.14, \mu_a = 0.09, \mu_m = 0.09, v = 10^{-7}, N = 10^7$ . For (A) we set  $u = 0$ , for (B)  $\lambda_a = 0.065, u = 10^{-2}$ , for (C)  $\lambda_a = 0.0899, u = 10^{-2}$  and for (D)  $\lambda_a = 0.095, u = 10^{-2}$ .

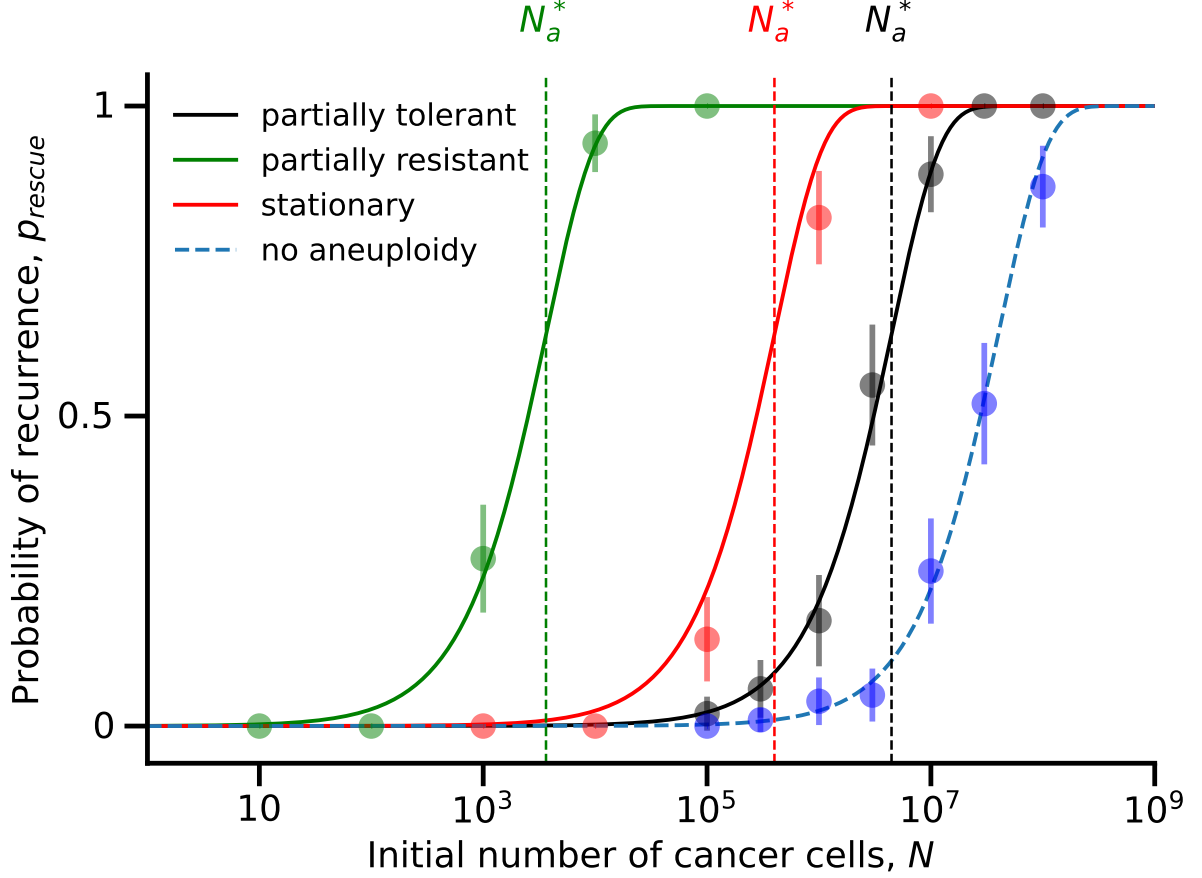
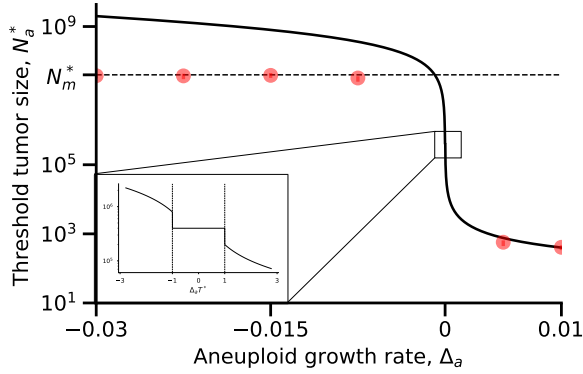


**Figure 3: Aneuploidy facilitates evolutionary rescue of cancer under drug treatment.** The probability of evolutionary rescue (i.e. the probability that the population does not go to extinction),  $p_{\text{rescue}}$ , as a function of the initial tumor size,  $N$  (see eq. (2)). Dashed vertical line shows the threshold tumor size,  $N_a^*$ , above which the probability is very high (see eq. (4)). Blue dashed line represents the probability of evolutionary rescue as a function of  $N$  without aneuploidy ( $u = 0$ ). The black line represents the case with tolerant aneuploidy ( $u = 10^{-2}$ ,  $\lambda_a = 0.0899$ ), the red line represents the case with stationary aneuploidy ( $u = 10^{-2}$ ,  $\lambda_a = 0.08999$ ) and the green line represents the case with partially resistant aneuploidy ( $u = 10^{-2}$ ,  $\lambda_a = 0.095$ ). The dots represent simulations and the error bars represent 95% confidence interval of the form  $p \pm 1.96\sqrt{p(1-p)/n}$  where  $p$  is the fraction of simulations in which the tumor has adapted to the stress and  $n = 100$  is the number of simulations. Parameters:  $\lambda_w = 0.1$ ,  $\lambda_m = 0.1$ ,  $\mu_w = 0.14$ ,  $\mu_a = 0.09$ ,  $\mu_m = 0.09$ ,  $v = 10^{-7}$ .

A



B

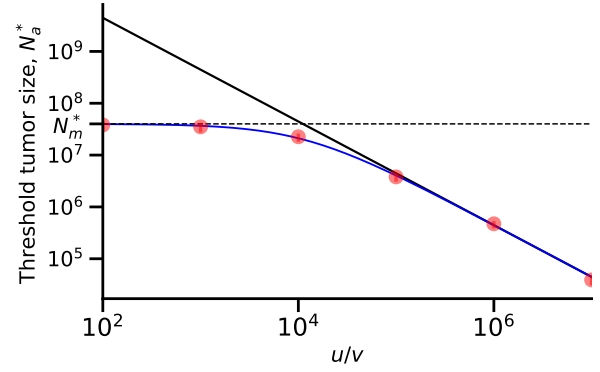


**Figure 4: Aneuploidy facilitates the evolutionary rescue of cancer under drug treatment.** (A) The threshold tumor size  $N_a^*$  as a function of the aneuploid growth rate  $\Delta_a$ . The dashed horizontal line shows  $N_m^*$ , the threshold tumor size without aneuploidy ( $u = 0$ ). When aneuploid growth rate is close to or higher than zero, aneuploidy decreases the threshold tumor size, thereby facilitating evolutionary rescue. The inset highlights the case when aneuploidy cancer cells are non-growing. The red dots represents simulations and the error bars represent the 95% confidence intervals obtained with bootstrapping, see Appendix G. Parameters:  $\lambda_w = 0.1, \lambda_m = 0.1, \mu_w = 0.14, \mu_a = 0.09, \mu_m = 0.09, u = 10^{-2}, v = 10^{-7}$ . (B) The threshold tumor size  $N_a^*$  as a function of the ratio of aneuploidy and mutation rates,  $u/v$ . The dashed horizontal line shows  $N_m^*$ , the threshold tumor size without aneuploidy ( $u = 0$ ). When the aneuploidy rate is much higher than the mutation rate, aneuploidy decreases the threshold tumor size, thereby facilitating evolutionary rescue. The blue line represents the exact formula for threshold tumor size  $N_a^*$  while the solid black line represents the approximation eq. (4). The red dots represents simulations and the error bars represent the 95% confidence intervals obtained with bootstrapping, see Appendix G. Parameters:  $\lambda_w = 0.1, \lambda_m = 0.0899, \lambda_m = 0.1, \mu_w = 0.14, \mu_a = 0.09, \mu_m = 0.09, v = 10^{-7}$ .

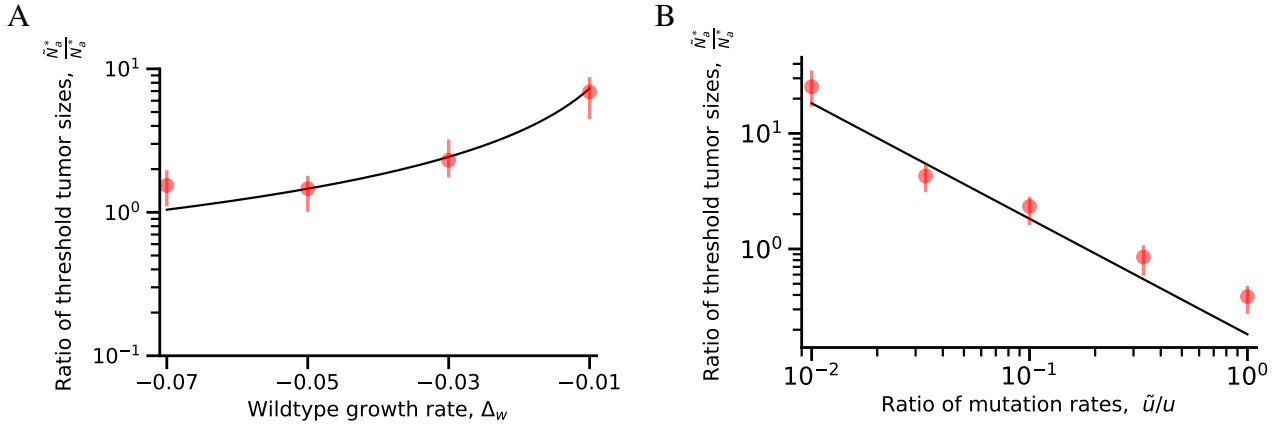


**Figure 5: Standing genetic variation facilitates evolutionary rescue of cancer under drug treatment.** (A) The ratio of threshold tumor size  $\tilde{N}_a^*$  when a fraction  $\frac{\tilde{u}\lambda_w}{s}$  is aneuploid at the start of treatment and  $N_a^*$  as a function of the wildtype growth rate  $\Delta_w$ . Standing genetic variation will drive adaptation to the drug if  $\Delta_w$  is very negative due to a stronger effect of the drug on sensitive cells. The red dots represents simulations and the error bars represent the 95% confidence intervals obtained with bootstrapping, see Appendix G. Parameters:  $\lambda_w = 0.1, \lambda_a = 0.0899, \lambda_m = 0.1, \mu_a = 0.09, \mu_m = 0.09, \tilde{u} = 10^{-3}, u = 10^{-2}, v = 10^{-7}$ . (B) The ratio of threshold tumor size  $\tilde{N}_a^*$  when a fraction  $\frac{\tilde{u}\lambda_w}{s}$  is aneuploid at the start of treatment and  $N_a^*$  as a function of the the ratio of aneuploidy rates  $\tilde{u}/u$ . De-novo aneuploids will have larger contribution to the appearance of drug resistance if the drug induces the appearance of aneuploid cells ( $u \gg \tilde{u}$ ). The red dots represents simulations and the error bars represent the 95% confidence intervals obtained with bootstrapping, see Appendix G. Parameters:  $\lambda_w = 0.1, \lambda_a = 0.0899, \lambda_m = 0.1, \mu_w = 0.14, \mu_a = 0.09, \mu_m = 0.09, \tilde{u} = 10^{-3}, v = 10^{-7}$ .

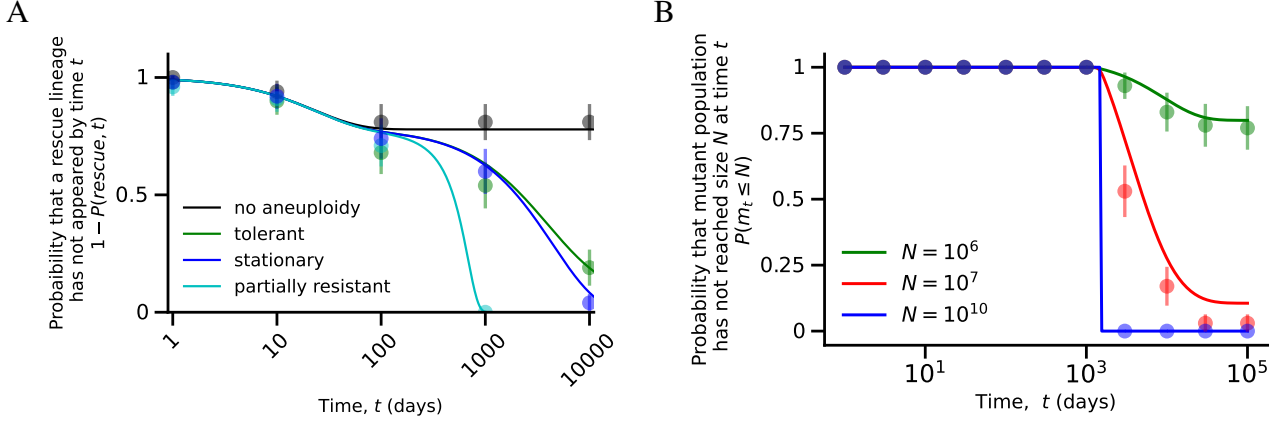


**Figure 6: Aneuploidy has a impact on cancer relapse early on.** (A) The probability that a successful mutant has not appeared by time  $t$ . The green line represents the case with tolerant aneuploidy ( $u > 0, \lambda_a = 0.0899$ ), the blue line represents the case with non-growing aneuploidy ( $u > 0, \lambda_a = 0.089999$ ), the cyan line represents the case with partially resistant aneuploidy ( $u > 0, \lambda_a = 0.095$ ) and the black line represents the case without aneuploidy ( $u = 0$ ). As time increases, aneuploidy plays an important role in helping the cancer cell population escape extinction. The markers represent simulations and the error bars represent 95% confidence interval of the form  $p \pm 1.96\sqrt{p(1-p)/n}$  where  $p$  is the fraction of simulations in which a successful mutant has not been generated and  $n = 100$  is the number of simulations. Parameters:  $\lambda_w = 0.1, \lambda_m = 0.1, \mu_w = 0.14, \mu_a = 0.09, \mu_m = 0.09, u = 10^{-2}, v = 10^{-7}, N = 10^7$ . (B) The probability that a mutant cancer cell population has not reached size  $N$  at time  $t$ . The green line represents the case where  $N = 10^6$  (small tumor), the red line represents  $N = 10^7$  (intermediate sized tumor) and the blue line represents the case where  $N = 10^{10}$  (large tumor). Increasing the initial tumor size guarantees that the tumor will regrow. The markers represent simulations and the error bars represents 95% confidence interval of the form  $p \pm 1.96\sqrt{p(1-p)/n}$  where  $p$  is the fraction of the simulations in which the mutant population size has not reached  $N$  and  $n = 100$  is the number of simulations. Parameters:  $\lambda_w = 0.1, \lambda_a = 0.0899, \lambda_m = 0.1, \mu_w = 0.14, \mu_a = 0.09, \mu_m = 0.09, u = 10^{-2}, v = 10^{-7}$ .

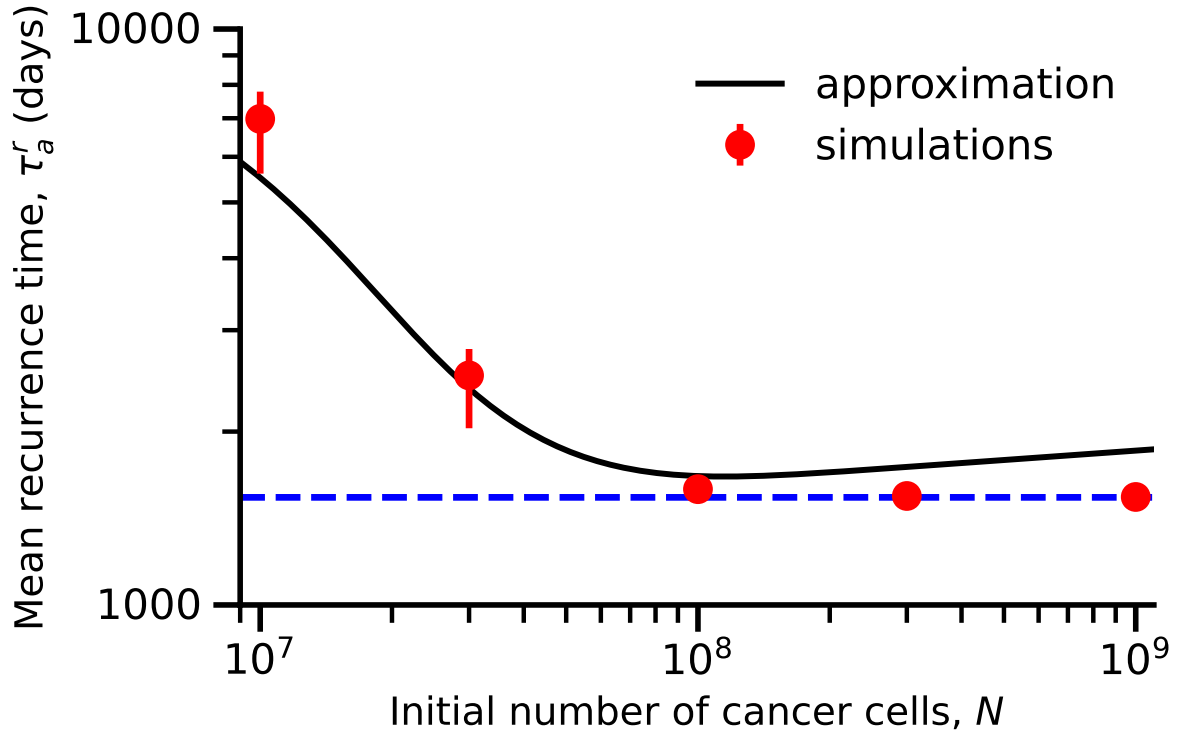


**Figure 7: Tumor size decreases the mean recurrence time.** The mean time for the mutant cell population to reach size  $N$ , the initial number of cancer cells. Our inhomogeneous Poisson-process approximation (solid black line, eq. (32)) is in agreement with simulation results (red markers with 95% confidence interval obtained with bootstrapping, see Appendix G) for intermediary  $N$ . The simulations converge to eq. (35) (blue dashed line) for large values of  $N$ . Parameters:  $\lambda_w = 0.1, \lambda_a = 0.0899, \lambda_m = 0.1, \mu_w = 0.14, \mu_a = 0.09, \mu_m = 0.09, u = 10^{-2}, v = 10^{-7}$ .

# Appendices

## Appendix A: Survival probability of a single lineage

To analyze evolutionary rescue in this model, we use the framework of *multitype branching processes* (Harris, 1963, Weissman et al., 2009). This allows us to find explicit expressions for the *survival probability*: the probability that a lineage descended from a single cell does not become extinct.

Let  $p_w$ ,  $p_a$ , and  $p_m$  be the survival probabilities of a population consisting initially of single wildtype cell, aneuploid cell, or mutant cell, respectively. The complements  $1 - p_w$ ,  $1 - p_a$ , and  $1 - p_m$  are the extinction probabilities, which satisfy each its respective equation (Harris, 1963),

$$\begin{aligned} 1 - p_w &= \frac{\mu_w}{\lambda_w + \mu_w + u\lambda_w + v\lambda_w} + \frac{u\lambda_w}{\lambda_w + \mu_w + u\lambda_w + v\lambda_w} (1 - p_a) (1 - p_w) + \\ &\quad \frac{\lambda_w}{\lambda_w + \mu_w + u\lambda_w + v\lambda_w} (1 - p_w)^2 + \frac{v\lambda_w}{\lambda_w + \mu_w + u\lambda_w + v\lambda_w} (1 - p_m) (1 - p_w), \\ 1 - p_a &= \frac{\mu_a}{\lambda_a + \mu_a + v\lambda_a} + \frac{v\lambda_a}{\lambda_a + \mu_a + v\lambda_a} (1 - p_m) (1 - p_a) + \frac{\lambda_a}{\lambda_a + \mu_a + v\lambda_a} (1 - p_a)^2, \\ 1 - p_m &= \frac{\mu_m}{\lambda_m + \mu_m} + \frac{\lambda_m}{\lambda_m + \mu_m} (1 - p_m)^2. \end{aligned} \quad (10)$$

The survival probabilities are given by the smallest solution for each quadratic equation (Uecker et al., 2015). Therefore we have

$$\begin{aligned} p_w &= \frac{\lambda_w - \mu_w - u\lambda_w p_a - v\lambda_w p_m + \sqrt{(\lambda_w - \mu_w - u\lambda_w p_a - v\lambda_w p_m)^2 + 4\lambda_w^2 (u p_a + v p_m)}}{2\lambda_w}, \\ p_a &= \frac{\lambda_a - \mu_a - v\lambda_a p_m + \sqrt{(\lambda_a - \mu_a - v\lambda_a p_m)^2 + 4\lambda_a^2 v p_m}}{2\lambda_a}, \\ p_m &= \frac{\lambda_m - \mu_m}{\lambda_m}. \end{aligned} \quad (11)$$

Note that the equation for  $p_w$  depends on both  $p_a$  and  $p_m$ , and the equation for  $p_a$  depends on  $p_m$ . To proceed, we can plug the solution for  $p_m$  and  $p_a$  into the solution for  $p_w$ . We perform this for three different scenarios.

### Scenario 1: Aneuploid cells are partially resistant

We first assume that aneuploidy provides partial resistance to drug therapy,  $\lambda_a > \mu_a$ , and that this resistance is significant,  $(\lambda_a - \mu_a - v\lambda_a p_m)^2 > 4\lambda_a^2 v p_m$ . We thus rewrite eq. (11) as

$$\begin{aligned} p_w &= \frac{\lambda_w - \mu_w - u\lambda_w p_a - v\lambda_w p_m}{2\lambda_w} \left( 1 - \sqrt{1 + \frac{4\lambda_w^2 (v p_m + u p_a)}{(\lambda_w - \mu_w - u\lambda_w p_a - v\lambda_w p_m)^2}} \right), \text{ and} \\ p_a &= \frac{\lambda_a - \mu_a - v\lambda_a p_m}{2\lambda_a} \left( 1 + \sqrt{1 + \frac{4\lambda_a^2 v p_m}{(\lambda_a - \mu_a - v\lambda_a p_m)^2}} \right). \end{aligned}$$

Using the quadratic Taylor expansion  $\sqrt{1+x} = 1 + x/2 + O(x^2)$  and assuming  $u, v \ll 1$ , we obtain the following approximation for the survival probability of a population initially consisting of a single wildtype cell,

$$p_w \approx -\frac{v\lambda_w p_m + u\lambda_w p_a}{\lambda_w - \mu_w - u\lambda_w p_a - v\lambda_w p_m} \quad (12)$$



$$\approx -\frac{1}{\lambda_w - \mu_w} \left[ \frac{u\lambda_w(\lambda_a - \mu_a)}{\lambda_a} + \frac{uv\lambda_w\lambda_a(\lambda_m - \mu_m)}{\lambda_m(\lambda_a - \mu_a)} + \frac{v\lambda_w(\lambda_m - \mu_m)}{\lambda_m} \right].$$

Now  $uv$  is very small, and if we use the fact that  $v \ll u$ , we have:

$$p_w \approx \frac{u\lambda_w}{|\Delta_w|} \cdot \frac{\Delta_a}{\lambda_a}. \quad (13)$$

However, if aneuploidy is very rare such that

$$\frac{u\lambda_w\Delta_a}{\lambda_a} < \frac{v\lambda_w\Delta_m}{\lambda_m} \Rightarrow u\lambda_a < \frac{v\lambda_a^2\Delta_m}{\lambda_m} \cdot \frac{1}{\Delta_a} < \frac{v\lambda_a^2\Delta_m}{\lambda_m} \cdot \frac{1}{\sqrt{4\lambda_a^2vp_m}} \Rightarrow u\lambda_a < T^*,$$

where  $T^* = (4v\lambda_a^2\Delta_m/\lambda_m)^{-1/2}$  and in the second inequality we used the fact that  $\Delta_a^2 > 4\lambda_a^2vp_m$ . In this case adaptation is through direct mutation and:

$$p_w \approx \frac{v\lambda_w}{|\Delta_w|} \cdot \frac{\Delta_m}{\lambda_m}.$$

## Scenario 2: Aneuploid cells are tolerant.

We now assume that aneuploidy provides tolerance to drug therapy, that is, the number of aneuploid cells significantly declines over time, but at a lower rate than the number of wildtype cells,  $\lambda_w - \mu_w < \lambda_a - \mu_a < 0$ . We also assume that the decline are significant,  $(\lambda_a - \mu_a - v\lambda_ap_m)^2 > 4\lambda_a^2vp_m$ . We rewrite eq. (11) as

$$\begin{aligned} p_w &= \frac{\lambda_w - \mu_w - u\lambda_wp_a - v\lambda_wp_m}{2\lambda_w} \left( 1 - \sqrt{1 + \frac{4\lambda_w^2(vp_m + up_a)}{(\lambda_w - \mu_w - u\lambda_wp_a - v\lambda_wp_m)^2}} \right), \\ p_a &= \frac{\lambda_a - \mu_a - v\lambda_ap_m}{2\lambda_a} \left( 1 - \sqrt{1 + \frac{4\lambda_a^2vp_m}{(\lambda_a - \mu_a - v\lambda_ap_m)^2}} \right). \end{aligned} \quad (14)$$

Since  $u, v \ll 1$ , the term in the root can be approximated using a 1st-order Taylor expansion. So, substituting the expressions for  $p_a$  and  $p_m$ , we have

$$\begin{aligned} p_w &\approx -\frac{v\lambda_wp_m + u\lambda_wp_a}{\lambda_w - \mu_w - u\lambda_wp_a - v\lambda_wp_m} \\ &\approx \frac{1}{\lambda_w - \mu_w - u\lambda_wp_a - v\lambda_wp_m} \left[ \frac{uv\lambda_w\lambda_a(\lambda_m - \mu_m)}{\lambda_m(\lambda_a - \mu_a - v\lambda_a)} - \frac{v\lambda_w(\lambda_m - \mu_m)}{\lambda_m} \right] \\ &\approx \frac{v\lambda_w(\lambda_m - \mu_m)}{\lambda_m(\lambda_w - \mu_w)} \left[ \frac{u\lambda_a}{(\lambda_a - \mu_a)} - 1 \right] \\ &= \frac{v\lambda_w\Delta_m}{\lambda_m|\Delta_w|} \left( \frac{u\lambda_a}{|\Delta_a|} + 1 \right). \end{aligned} \quad (15)$$

If we assume that  $u\lambda_a > |\Delta_a|$  then we have:

$$p_w \approx \frac{u\lambda_w}{|\Delta_w|} \cdot \frac{v\lambda_a}{|\Delta_a|} \cdot \frac{\Delta_m}{\lambda_m}. \quad (16)$$

### Scenario 3: Aneuploid cells are stationary

We now assume that the growth rate of aneuploid cells is close to zero (either positive or negative), such that  $(\Delta_a - v\lambda_a p_m)^2 \ll 4\lambda_a^2 v p_m$ . We rewrite eq. (11) as

$$p_a = \frac{\lambda_a - \mu_a - v\lambda_a p_m + 2\sqrt{\lambda_a^2 v p_m} \left(1 + \frac{(\lambda_a - \mu_a - v\lambda_a p_m)^2}{4\lambda_a^2 v p_m}\right)^{\frac{1}{2}}}{2\lambda_a}. \quad (17)$$

Using a following Taylor series expansion for small  $(\lambda_a - \mu_a - v\lambda_a p_m)^2 / 4\lambda_a^2 v p_m$ ,

$$\left(1 + \frac{(\lambda_a - \mu_a - v\lambda_a p_m)^2}{4\lambda_a^2 v p_m}\right)^{\frac{1}{2}} = 1 + \frac{(\lambda_a - \mu_a - v\lambda_a p_m)^2}{8\lambda_a^2 v p_m} + \dots,$$

we obtain the approximation

$$\begin{aligned} p_a &\approx \frac{\lambda_a - \mu_a - v\lambda_a p_m + 2\sqrt{\lambda_a^2 v p_m} \left[1 + \frac{(\lambda_a - \mu_a - v\lambda_a p_m)^2}{8\lambda_a^2 v p_m}\right]}{2\lambda_a} \\ &= \frac{\lambda_a - \mu_a - v\lambda_a p_m + 2\sqrt{\lambda_a^2 v p_m} + \frac{(\lambda_a - \mu_a - v\lambda_a p_m)^2}{4\sqrt{\lambda_a^2 v p_m}}}{2\lambda_a} \\ &= \frac{(\lambda_a - \mu_a - v\lambda_a p_m + 2\sqrt{\lambda_a^2 v p_m})^2 + 4\lambda_a^2 v p_m}{8\lambda_a \sqrt{\lambda_a^2 v p_m}} \\ &= \frac{4\lambda_a^2 v p_m + 4\lambda_a^2 v p_m \left(1 + \frac{\lambda_a - \mu_a - v\lambda_a p_m}{2\sqrt{\lambda_a^2 v p_m}}\right)^2}{8\lambda_a \sqrt{\lambda_a^2 v p_m}} \\ &= \frac{1}{2\lambda_a} \left(\lambda_a - \mu_a - v\lambda_a p_m + 2\sqrt{\lambda_a^2 v p_m}\right). \end{aligned} \quad (18)$$

Plugging this in eq. (12), the survival probability of a population starting from one wildtype individual is

$$\begin{aligned} p_w &\approx -\frac{1}{\lambda_w - \mu_w - u\lambda_w p_a - v\lambda_w p_m} \left[ v\lambda_w \frac{\lambda_m - \mu_m}{\lambda_m} + \frac{u\lambda_w}{2\lambda_a} \left(\lambda_a - \mu_a - v\lambda_a p_m + 2\sqrt{\lambda_a^2 v p_m}\right) \right] \\ &= -\frac{1}{\lambda_w - \mu_w - u\lambda_w - v\lambda_w} \left[ v\lambda_w \frac{\lambda_m - \mu_m}{\lambda_m} + \frac{u\lambda_w}{2\lambda_a} (\lambda_a - \mu_a - v\lambda_a p_m) + u\lambda_w \sqrt{\frac{v(\lambda_m - \mu_m)}{\lambda_m}} \right] \\ &\approx -\frac{1}{\Delta_w} \left[ v\lambda_w \frac{\Delta_m}{\lambda_m} + \frac{u\lambda_w (\Delta_a - v\lambda_a)}{2\lambda_a} + u\lambda_w \sqrt{\frac{v\Delta_m}{\lambda_m}} \right]. \end{aligned} \quad (19)$$

Using the fact that

$$(\Delta_a - v\lambda_a p_m)^2 \ll 4\lambda_a^2 v p_m \Rightarrow \frac{\Delta_a - v\lambda_a p_m}{2\lambda_a} \ll \sqrt{\frac{v\lambda_a \Delta_m}{\lambda_m}},$$

and  $v \ll u$  we obtain:

$$p_w \approx \frac{u\lambda_w}{|\Delta_w|} \cdot \sqrt{\frac{v\lambda_a \Delta_m}{\lambda_m}}. \quad (20)$$

## Appendix B: Evolutionary rescue probability

Using the fact that  $\Delta_a - v\lambda_a p_m \approx \Delta_a$  we write the condition  $(\Delta_a - v\lambda_a p_m)^2 \ll 4\lambda_a^2 v p_m$  as:

$$\Delta_a^2 \ll 4\lambda_a^2 v p_m \Rightarrow -1 \ll \Delta_a T^* \ll 1,$$

where  $T^* = (4v\lambda_a^2 \Delta_m / \lambda_m)^{-1/2}$ . Substituting eqs. (13), (16) and (20) into eq. (2), the evolutionary rescue probability can be approximated by

$$p_{\text{rescue}} \approx \begin{cases} 1 - \exp\left[-\frac{u\lambda_a}{|\Delta_w|} \cdot \frac{v\lambda_w}{|\Delta_a|} \cdot \frac{\Delta_m}{\lambda_m} \cdot N\right], & \Delta_a T^* \ll -1, \\ 1 - \exp\left[-\frac{u\lambda_w}{|\Delta_w|} \cdot \sqrt{\frac{v\lambda_a \Delta_m}{\lambda_m}} \cdot N\right], & -1 \ll \Delta_a T^* \ll 1, \\ 1 - \exp\left[-\frac{u\lambda_w}{|\Delta_w|} \cdot \frac{\Delta_a}{\lambda_a} \cdot N\right], & 1 \ll \Delta_a T^*. \end{cases} \quad (21)$$

## Appendix C: Evolutionary rescue time

We first calculate the expected time for the appearance of the first mutant that rescues the cell population. This can occur either through the evolutionary trajectory *wildtype*  $\rightarrow$  *mutant* or through the trajectory *wildtype*  $\rightarrow$  *aneuploid*  $\rightarrow$  *mutant*. We start with the former.

Assuming no aneuploidy ( $u = 0$ ), we define  $T_m$  to be the time at which the first mutant cell appears that will avoid extinction and will therefore rescue the population. Note that if extinction occurs, that is the frequency of mutants after a very long time is zero,  $m_\infty = 0$ , then it is implied that  $T_m = \infty$ , and vice versa if  $T_m < \infty$  then  $m_\infty > 0$ .

The number of successful mutants generated until time  $t$  can be approximated by an inhomogeneous Poisson process with rate  $R_m(t) = v\lambda_w p_m w_t$ , where  $w_t = Ne^{\Delta_w t}$  is the number of wildtype cells at time  $t$ . Note that

$$\int_0^t R_m(z) dz = v\lambda_w p_m N \frac{\exp[\Delta_w t] - 1}{\Delta_w} \approx v\lambda_w p_m N t, \quad (22)$$

by integrating the exponential and because  $\frac{\exp[\Delta_w t] - 1}{\Delta_w} = \frac{1 + \Delta_w t + O(t^2) - 1}{\Delta_w} = t + O(t^2)$ . The probability density function of  $T_m$  is thus  $R_m(t) \exp\left(-\int_0^t R_m(z) dz\right)$  (Allen, 2010). Therefore, the probability density function of the conditional random variable  $(T_m | T_m < \infty)$  is  $f_m(t) = \frac{R_m(t) \exp\left(-\int_0^t R_m(z) dz\right)}{p_{\text{rescue}}}$ .

We are interested in the mean conditional time,  $\tau_m = \mathbb{E}[T_m | T_m < \infty]$ , which is given by

$$\tau_m = \int_0^\infty t f_m(t) dt = \frac{\int_0^\infty t R_m(t) \exp\left(-\int_0^t R_m(z) dz\right) dt}{p_{\text{rescue}}}, \quad (23)$$

Therefore, plugging eqs. (22) and (2) in eq. (23),

$$\tau_m = \int_0^\infty t v\lambda_w N e^{\Delta_w t} \frac{e^{-v\lambda_w N p_m \frac{e^{\Delta_w t} - 1}{\Delta_w}}}{1 - (1 - p_w)^N} dt \approx \int_0^\infty t v\lambda_w N e^{\Delta_w t} \frac{e^{-v\lambda_w N p_m t}}{1 - e^{-N p_w}} dt. \quad (24)$$

Figure 9B show the agreement between this approximating and simulation results.

Assuming aneuploidy is possible ( $u > 0$ ), we define  $T_a$  to be the time at which the first mutant cell appears that will rescue the population. We are interested in the mean conditional time,  $\tau_a = \mathbb{E}[T_a | T_a < \infty]$ .

When  $Nu\lambda_w/|\Delta_w| \gg 1$  the aneuploid frequency dynamics is roughly deterministic and therefore can be approximated by

$$a_t \approx \frac{Nu\lambda_w e^{\Delta_w t}}{\Delta_w - \Delta_a} \left[ 1 - e^{-(\Delta_w - \Delta_a)t} \right]. \quad (25)$$

As a result, the number of successful mutants created by direct mutation and via aneuploidy can be approximated by inhomogeneous Poisson processes with the rates

$$r_1(t) = v\lambda_a p_m \int_0^t a_z dz = \frac{uv\lambda_w \lambda_a N p_m}{\Delta_w - \Delta_a} \left( \frac{e^{\Delta_w t} - 1}{\Delta_w} - \frac{e^{\Delta_a t} - 1}{\Delta_a} \right), \quad (26)$$

$$r_2(t) = v\lambda_w p_m \int_0^t w_z dz = v\lambda_w N p_m \frac{e^{\Delta_w t} - 1}{\Delta_w}. \quad (27)$$

For large initial population sizes we assume that the two processes are independent and as a result, they can be merged into a single Poisson process with rate  $R_a(t) = (r_1 + r_2)(t)$ . Consequently, the mean time to the appearance of the first rescue mutant is

$$\begin{aligned} \tau_a &= \frac{\int_0^\infty t R_a(t) \exp\left(-\int_0^t R_a(z) dz\right) dt}{p_{rescue}} \\ &= \int_0^\infty t (v\lambda_a p_m a_t + v\lambda_w p_m w_t) \frac{\exp\left[-\frac{uv\lambda_w \lambda_a N p_m}{\Delta_w - \Delta_a} \left(\frac{e^{\Delta_w t} - 1}{\Delta_w} - \frac{e^{\Delta_a t} - 1}{\Delta_a}\right) - v\lambda_w N p_m \frac{e^{\Delta_w t} - 1}{\Delta_w}\right]}{1 - e^{-N p_w}} dt, \end{aligned} \quad (28)$$

which we plot in Figure 9A as a function of the initial population size,  $N$ .

Paradoxically, we observe from Figure 9 that the mean time of a rescue mutation to appear is significantly shorter for the case when  $u = 0$  when compared to the case  $u > 0$ , however this can be explained by the fact this mean time is conditioned on evolutionary rescue and, as a result, aneuploidy increase the *window of opportunity* in which a rescue mutation could appear thus increasing the mean time as well (Figure 2).

If  $N \gg N_m^*$  then the mean time  $\tau_a$  can be written as:

$$\tau_a = \int_0^\infty e^{-R_a(\tau)} d\tau = \int_0^\infty \exp\left[-\frac{uv\lambda_w \lambda_a N p_m}{\Delta_w - \Delta_a} \left(\frac{e^{\Delta_w \tau} - 1}{\Delta_w} - \frac{e^{\Delta_a \tau} - 1}{\Delta_a}\right) - v\lambda_w N p_m \frac{e^{\Delta_w \tau} - 1}{\Delta_w}\right] d\tau,$$

and we use the following Taylor series expansions:

$$\begin{aligned} \frac{e^{\Delta_w \tau} - 1}{\Delta_w} &= \frac{1 + \Delta_w \tau + O(\tau^2) - 1}{\Delta_w} = \tau + O(\tau^2). \\ \frac{e^{\Delta_a \tau} - 1}{\Delta_a} &= \frac{1 + \Delta_a \tau + O(\tau^2) - 1}{\Delta_a} = \tau + O(\tau^2), \end{aligned}$$

to obtain a simpler approximation for  $\tau_a$ :

$$\tau_a \approx \int_0^\infty e^{-v\lambda_w N p_m \tau} d\tau = \frac{1}{v\lambda_w N p_m}. \quad (29)$$

If  $N \ll N_a^*$  then we can write Equation (28) as:

$$\tau_a \approx \frac{\int_0^\infty t v\lambda_a p_m a_\tau d\tau}{1 - e^{-N p_w}} \approx \frac{uv\lambda_a \lambda_w p_m |\Delta_w + \Delta_a|}{p_w \Delta_a^2 \Delta_w^2}$$

$$= \frac{1}{|\Delta_w|} + \frac{1}{|\Delta_a|}, \quad (30)$$

where in the last line we used the fact that  $1/p_w = N_a^*$  and Equation (4).

If a fraction  $f$  of the cancer cells are aneuploid when the drug is administered then the rates at which the rescue mutations are generated can be written as:

$$r_1^f(t) = v\lambda_a p_m \int_0^t a_z dz = (1-f) \frac{uv\lambda_w \lambda_a N p_m}{\Delta_w - \Delta_a} \left( \frac{e^{\Delta_w t} - 1}{\Delta_w} - \frac{e^{\Delta_a t} - 1}{\Delta_a} \right) + f v\lambda_a N p_m \frac{e^{\Delta_a t} - 1}{\Delta_a},$$

$$r_2^f(t) = v\lambda_w p_m \int_0^t w_z dz = (1-f) v\lambda_w N p_m \frac{e^{\Delta_w t} - 1}{\Delta_w},$$

and the mean evolutionary rescue time is given by:

$$\tau_a = \frac{\int_0^\infty t R_a^f(t) \exp\left(-\int_0^t R_a^f(z) dz\right) dt}{p_{\text{rescue}}}, \quad (31)$$

where  $R_a^f(t) = r_1^f(t) + r_2^f(t)$  and  $p_{\text{rescue}} = 1 - \exp[-(1-f)p_w N - f p_a N]$ . We plot our approximation in Figure 16 together with simulated data.

## Appendix D: Recurrence time

We define the proliferation time  $\tau_a^r$  to be the time it takes the population of mutant cancer cells to reach the initial tumor size  $N$ . The number of rescue lineages generated by the wildtype population is given by eq. (26) (see Figure 10):

$$r_1(\infty) = \frac{uv\lambda_w \lambda_a N p_m}{|\Delta_w| |\Delta_a|} = \frac{N}{N_a^*},$$

where we ignore lineages created by direct mutation because we assumed  $u\lambda_a > \max(-\Delta_a, 1/T^*)$ ,  $N \ll N_m^*$  and used Equation (4).

This helps us distinguish between two cases for the proliferation time. Firstly, when we have at most one lineages which rescues the cancer cell population:

$$N \ll N_a^*.$$

As a result, the recurrence time is given by (Avanzini and Antal, 2019):

$$\tau_a^r \approx \tau_a + \frac{\log p_m N}{\Delta_m}. \quad (32)$$

The factor of  $p_m$  in the second term of eq. (32) is due to the fact that the lineage is conditioned to survive genetic drift and the time to reach  $N$  is shorter then the case without this property.

The second case is when the wildtype population produces a large number of rescue lineages in a short period of time. This is given by the condition:

$$N \gg N_a^*.$$

As a result, the recurrence time is obtained by solving the following system of ODEs:

$$\begin{aligned} \frac{dw}{dt} &= \Delta_w w, \\ \frac{da}{dt} &= \Delta_a a + u\lambda_w w, \\ \frac{dm}{dt} &= \Delta_m m + v\lambda_a a + v\lambda_w w. \end{aligned} \quad (33)$$

Solving the system of ODEs for initial condition  $(w(0), a(0), m(0)) = (N, 0, 0)$  we obtain:

$$m(t) = \frac{Nuv\lambda_a\lambda_w}{\Delta_w - \Delta_a} \left[ \frac{e^{\Delta_w t} - e^{\Delta_m t}}{\Delta_w - \Delta_m} - \frac{e^{\Delta_a t} - e^{\Delta_m t}}{\Delta_a - \Delta_m} \right] + Nv\lambda_w \frac{e^{\Delta_w t} - e^{\Delta_m t}}{\Delta_w - \Delta_m}.$$

We obtain  $\tau_a^r$  such that  $m(\tau_a^r) = N$  by solving:

$$1 = \frac{uv\lambda_a\lambda_w}{\Delta_w - \Delta_a} \left[ \frac{e^{\Delta_w \tau_a^r} - e^{\Delta_m \tau_a^r}}{\Delta_w - \Delta_m} - \frac{e^{\Delta_a \tau_a^r} - e^{\Delta_m \tau_a^r}}{\Delta_a - \Delta_m} \right] + v\lambda_w \frac{e^{\Delta_w \tau_a^r} - e^{\Delta_m \tau_a^r}}{\Delta_w - \Delta_m}. \quad (34)$$

This is a transcendental equation which cannot be solved exactly but we can obtain an approximation by noting that for large  $\tau_a^r$  the above equation can be written as:

$$1 = v\lambda_w \frac{e^{\Delta_m \tau_a^r}}{|\Delta_w - \Delta_m|},$$

which has solution:

$$\tau_a^r \approx \frac{1}{\Delta_m} \log \frac{\Delta_m - \Delta_w}{v\lambda_w}. \quad (35)$$

We observe that the terms given by the evolutionary trajectory *wildtype*  $\rightarrow$  *aneuploid*  $\rightarrow$  *mutant* do not contribute to the above approximation and, as a result, we deduce that it accurate only for  $N \gg N_m^* > N_a^*$ .

Additionally, we note that if we are interested in the time until the tumor reaches a detectable size  $M$  then our above analysis is valid but in Equation (32) we change:

$$\tau_a^{r,M} \approx \tau_a + \frac{\log p_m M}{\Delta_m}, \quad (36)$$

and Equation (35) becomes:

$$\tau_a^{r,M} \approx \frac{1}{\Delta_m} \log \frac{M(\Delta_m - \Delta_w)}{v\lambda_w N}, \quad (37)$$

which we plot in Figure 15 and observe that our approximations are in agreement with simulations.

## Appendix E: Distribution of evolutionary rescue time

The probability that a successful mutant has been generated by time  $t$  is given by:

$$\begin{aligned} P(\text{rescue}, t) &= P(T_a < t) \\ &= 1 - \exp \left\{ - [r_1(t) + r_2(t)] \right\} \\ &= 1 - \exp \left\{ - \left[ \frac{uv\lambda_w\lambda_a N p_m}{\Delta_w - \Delta_a} \left( \frac{e^{\Delta_w t} - 1}{\Delta_w} - \frac{e^{\Delta_a t} - 1}{\Delta_a} \right) + v\lambda_w N p_m \frac{e^{\Delta_w t} - 1}{\Delta_w} \right] \right\}, \end{aligned}$$

where  $T_a$  is the time at which the first mutant cell appears that will avoid extinction and which was defined in Appendix C.

As a result, the probability that a successful mutant has not been generated by time  $t$  is:

$$1 - P(\text{rescue}, t) = \exp \left\{ - \left[ \frac{uv\lambda_w\lambda_a N p_m}{\Delta_w - \Delta_a} \left( \frac{e^{\Delta_w t} - 1}{\Delta_w} - \frac{e^{\Delta_a t} - 1}{\Delta_a} \right) + v\lambda_w N p_m \frac{e^{\Delta_w t} - 1}{\Delta_w} \right] \right\}. \quad (38)$$

## Appendix F: Distribution of recurrence time

The probability distribution of the time that a lineage, consisting initially of a single cell, will reach size  $N$  as time  $t$  is given by the Gumbel distribution  $\text{Gumb}_{\max}\left(\frac{\log N p_m}{\Delta_m}, \frac{1}{\Delta_m}\right)$  (Avanzini and Antal, 2019) with probability density function:

$$G(t) = e^{-p_m N e^{-\Delta_m t}}.$$

A mutant lineage initiated at time  $s$ , through aneuploidy, at rate  $v\lambda_a p_m a_s$  reaches size  $N$  before time  $t$  with probability  $G(t - s)$  where  $s \leq t$ . As a result, the number of successful mutant lineages which reach size  $N$  by time  $t$  can be approximated by inhomogeneous Poisson random variable with rate:

$$r(t) = v\lambda_a p_m \int_0^t a_s G(t - s) ds$$

where  $a_s$  is aneuploid population size at time  $s$  defined in eq. (25). The proliferation time is defined as the first time the size of all lineages reaches  $N$ . When  $N \ll |\Delta_w||\Delta_a|/uv\lambda_w\lambda_a p_m$  there is at most a single mutant lineage that will survive and reach size  $N$  (Figure 10) and the probability that the size of that lineage has not reached  $N$  by time  $t$  is given by:

$$\begin{aligned} P(m_t \leq N) &= \exp[-r(t)] \\ &= \exp\left[-\frac{Nuv\lambda_w\lambda_a p_m}{\Delta_w - \Delta_a} \int_0^t \left[e^{\Delta_w s} - e^{\Delta_a s}\right] e^{-p_m N e^{-\Delta_m(t-s)}} ds\right]. \end{aligned} \quad (39)$$

When  $N \gg |\Delta_w||\Delta_a|/uv\lambda_w\lambda_a p_m$  the dynamics of the cancer cell populations is deterministic and approximated by the system of ODEs shown in eq. (33). As a result, the size of the mutant cell population will always be below  $N$  until time  $\tau_a^r$  and will always be greater after:

$$P(m_t \leq N) = 1 - H(t - \tau_a^r), \quad (40)$$

where  $H(x)$  is the Heaviside function:

$$H(x) = \begin{cases} 0, & x < 0, \\ 1, & x \geq 0. \end{cases}$$

We plot eq. (39) and eq. (40) in Figure and compare with stochastic simulations and observe that our approximation are in agreement.

We observe that for  $N = 10^7$  our formula overestimates the probability that the mutant population will be smaller than  $N$  at time  $t$ . This can be explained by the fact that  $N = 10^7$  is an intermediary case where the wildtype population produces a number of rescue lineages that is greater than one but still sufficiently small such that stochasticity plays an important role in the population dynamics. As a result, the number of mutant cancer cells will reach  $N$  faster than the case with a single mutant lineage. Additionally, we observe from Figure 6B that the probability of the mutant cell population reaching size  $N$  is approximately zero before time  $\tau_a^r$  which is the recurrence time for the deterministic case. This can be explained as follows: in the deterministic case there is a sufficient number of lineages produced such that there exists a lineage where each descendant will only reproduce and not die; the time it takes for this lineage to reach  $N$  is the lower bound for the time of all other lineages to reach  $N$  and this time cannot be smaller than  $\tau_a^r$  by definition. Given that for small values of  $N$  we expect that at most a single lineage will rescue the tumor, this lineage cannot reach  $N$  before  $\tau_a^r$  for the deterministic case eq. (35).

From eq. (40) we obtain the distribution of the recurrence time conditional of evolutionary rescue:

$$f(t) = \frac{d}{dt} \left[ \frac{P(m_t \geq N)}{p_{\text{rescue}}} \right] = r'(t) \frac{\exp[-r(t)]}{p_{\text{rescue}}}, \quad (41)$$

which we plot in Figure and compare with simulations. We note that in the case  $N \gg |\Delta_w||\Delta_a|/uv\lambda_w\lambda_a p_m$  the distribution becomes the Dirac  $\delta$ -function (Barton, 1989).

## Appendix G: Bootstrapping

For the mean times the 95% confidence interval is obtained through bootstrapping in the following steps: (1) we simulate  $T$  100 times; (2) we sample with replacement which we store in  $T'$ ; (3) for each element of this sample we obtain  $\tau = \mathbb{E}[T']$ ; (4) we repeat steps (2)-(3) 100 times to obtain  $\tau$  and we select the upper and lower limits such that 95% of the values of  $\tau$  lie in the interval given by the bounds.

For the threshold tumor sizes the 95% confidence interval is obtained through bootstrapping in the following steps: (1) we simulate  $p_{rescue}$  100 times; (2) we sample with replacement which we store in  $S$ ; (3) for each element of this sample we obtain  $N_a^* = 1/p_w$  using  $p_w = -1/N_s \log(1 - \bar{S})$  where  $\bar{S}$  is the mean of  $S$  and  $N_s$  is an arbitrary value of the initial population size we selected in order to calculate  $p_{rescue}$ ; (4) we repeat steps (2)-(3) 100 times to obtain  $N_a^*$  and we select the upper and lower limits such that 95% of the values of  $N_a^*$  lie in the interval given by the bounds.

For the ratio of the threshold tumor sizes the 95% confidence interval is obtained through bootstrapping in the following steps: (1) we simulate  $p_{rescue}$  100 times for both the case when  $f = \tilde{u}\lambda_w/s$  and  $f = 0$ ; (2) we sample with replacement which we store in  $S_0$  and  $S_f$ ; (4) for each element of  $S_0$  we obtain  $N_a^* = 1/p_w$  using  $p_w = -1/N_s \log(1 - \bar{S})$  where  $\bar{S}$  is the mean of  $S_0$  and  $N_s$  is an arbitrary value of the initial population size we selected in order to calculate  $p_{rescue}$ ; (5) for each element of  $S_f$  we obtain  $\tilde{N}_a^* = 1/p_a$  using  $p_a = -f/N_s \log(1 - \bar{S})$  where  $\bar{S}_f$  is the mean of  $S_f$  and  $N_s$  is an arbitrary value of the initial population size we selected in order to calculate  $p_{rescue}$ ; (6) we repeat steps (2)-(5) 100 times to obtain  $\tilde{N}_a^*/N_a^*$  and we select the upper and lower limits such that 95% of the values of  $\tilde{N}_a^*/N_a^*$  lie in the interval given by the bounds.



## Appendix F: Figures

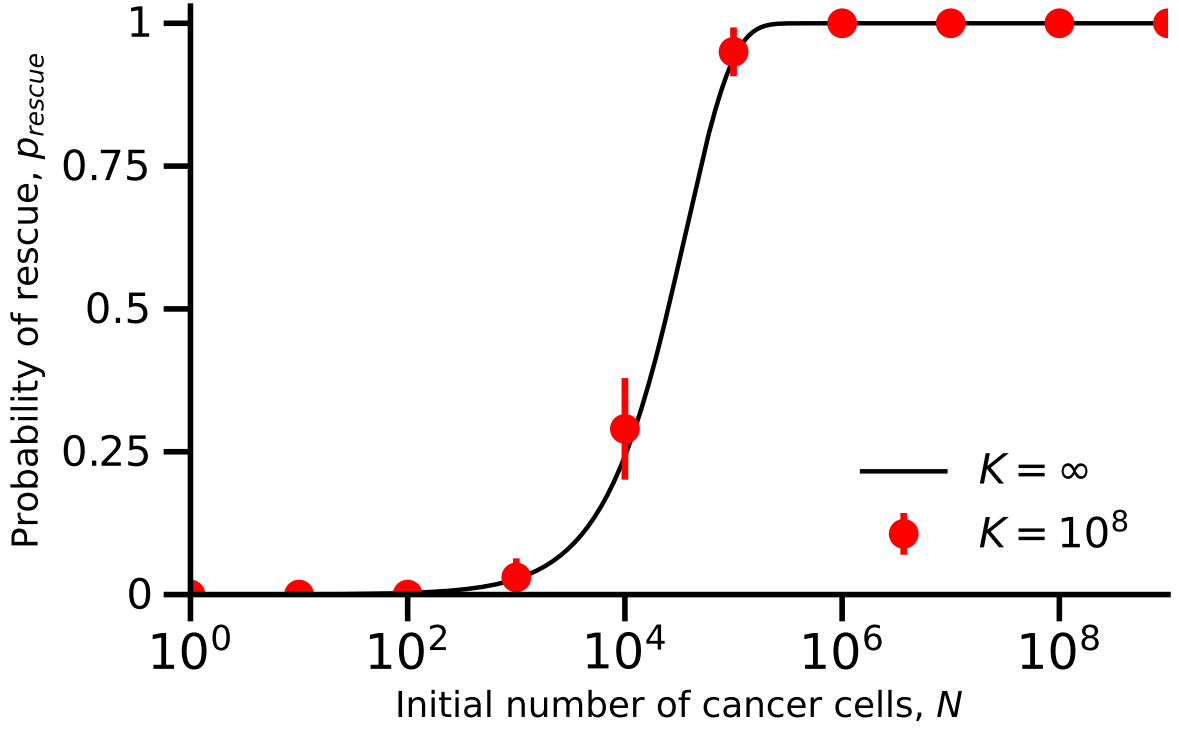


**Figure 8: Density dependent growth does not affect the accuracy of our model.** Comparison of results of simulations with density-dependent growth (red markers with 95% CI) and the approximation formula (black line, eq. (4) in eq. (2)) with maximum carrying capacity  $K = 10^8$  and effective carrying capacity  $K_e = K\Delta_a/\lambda_a \approx 10^6$ . The error bars represent 95% confidence interval of the form  $p \pm 1.96\sqrt{p(1-p)/n}$  where  $p$  is the fraction of simulations in which the tumor has adapted to the stress and  $n = 100$  is the number of simulations. Parameters:  $\lambda_w = 0.1, \lambda_a = 0.0901, \lambda_m = 0.1, \mu_w = 0.14, \mu_a = 0.09, \mu_m = 0.09, u = 10^{-2}, v = 10^{-7}, K = 10^8$ .

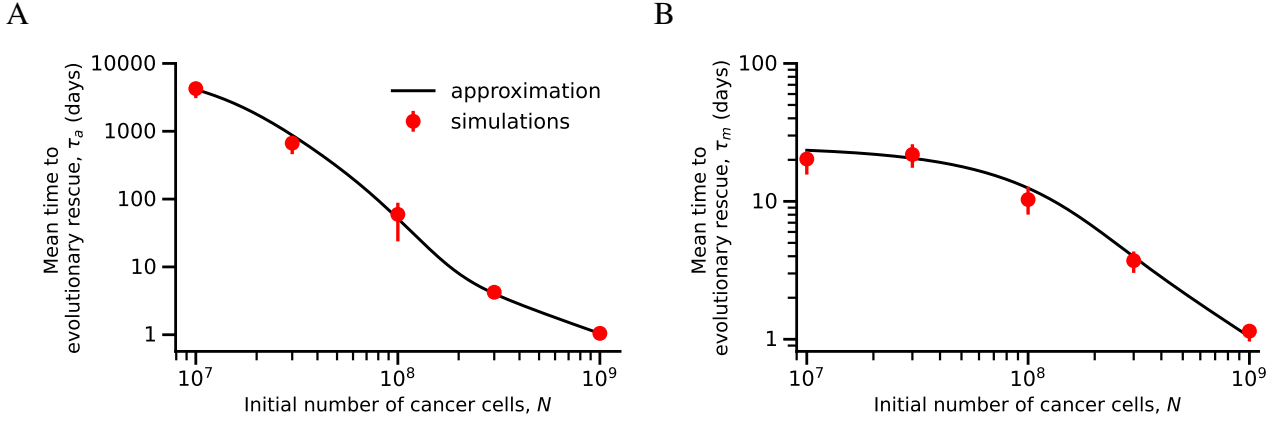


**Figure 9: Evolutionary rescue time.** Shown is the mean time for appearance of a resistance mutation the leads to evolutionary rescue (A) with aneuploidy ( $u > 0$ ) and (B) without aneuploidy ( $u = 0$ ). Our inhomogeneous Poisson-process approximations (solid black lines, right: eq. (23), left: eq. (28)) is in agreement with simulation results (red markers with 95% quantile intervals obtained with bootstrapping, see Appendix G). Parameters:  $\lambda_w = 0.1$ ,  $\lambda_m = 0.0899$ ,  $\lambda_m = 0.1$ ,  $\mu_w = 0.14$ ,  $\mu_a = 0.09$ ,  $\mu_m = 0.09$ ,  $u = 10^{-2}$ ,  $v = 10^{-7}$ .

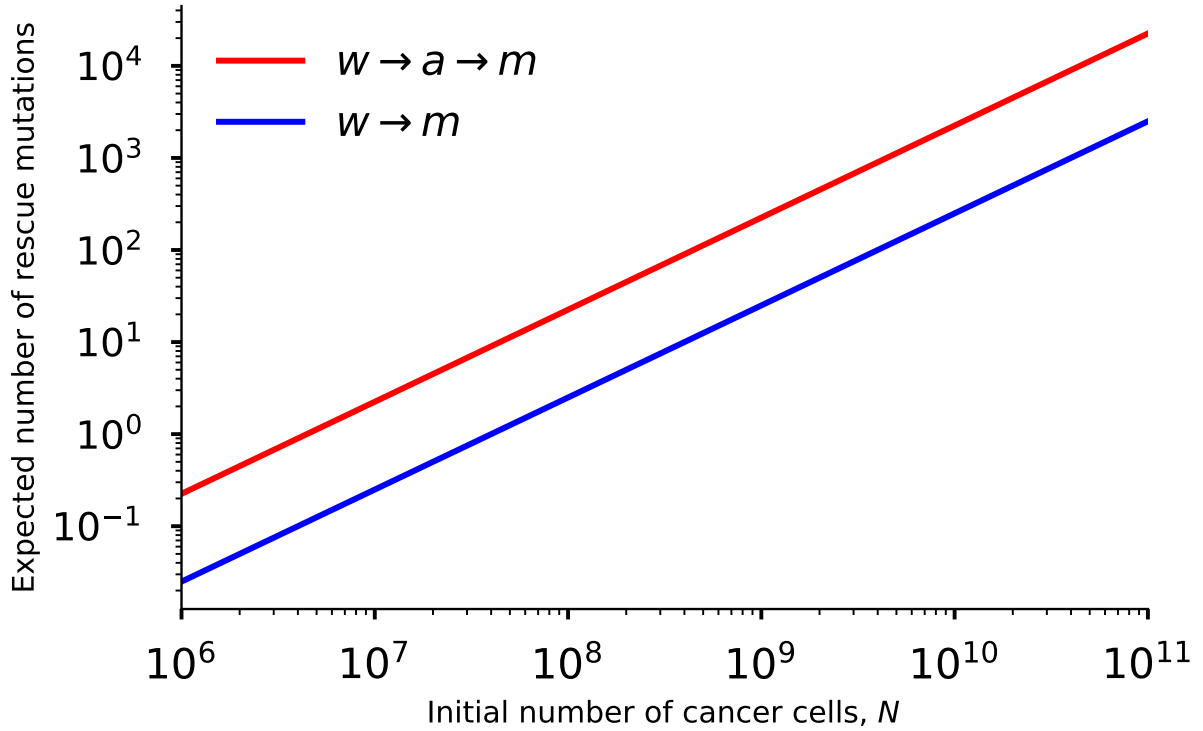


**Figure 10: Aneuploidy increases the number of mutations which rescue the tumor.** Shown is the expected number of mutation, which will rescue the cancer cell population, produced through the evolutionary trajectory *wildtype*  $\rightarrow$  *mutant* (blue line, eq. (27)) or through the trajectory *wildtype*  $\rightarrow$  *aneuploid*  $\rightarrow$  *mutant* (red line, eq. (26)). Parameters:  $\lambda_w = 0.1$ ,  $\lambda_m = 0.0899$ ,  $\lambda_m = 0.1$ ,  $\mu_w = 0.14$ ,  $\mu_a = 0.09$ ,  $\mu_m = 0.09$ ,  $u = 10^{-2}$ ,  $v = 10^{-7}$ .

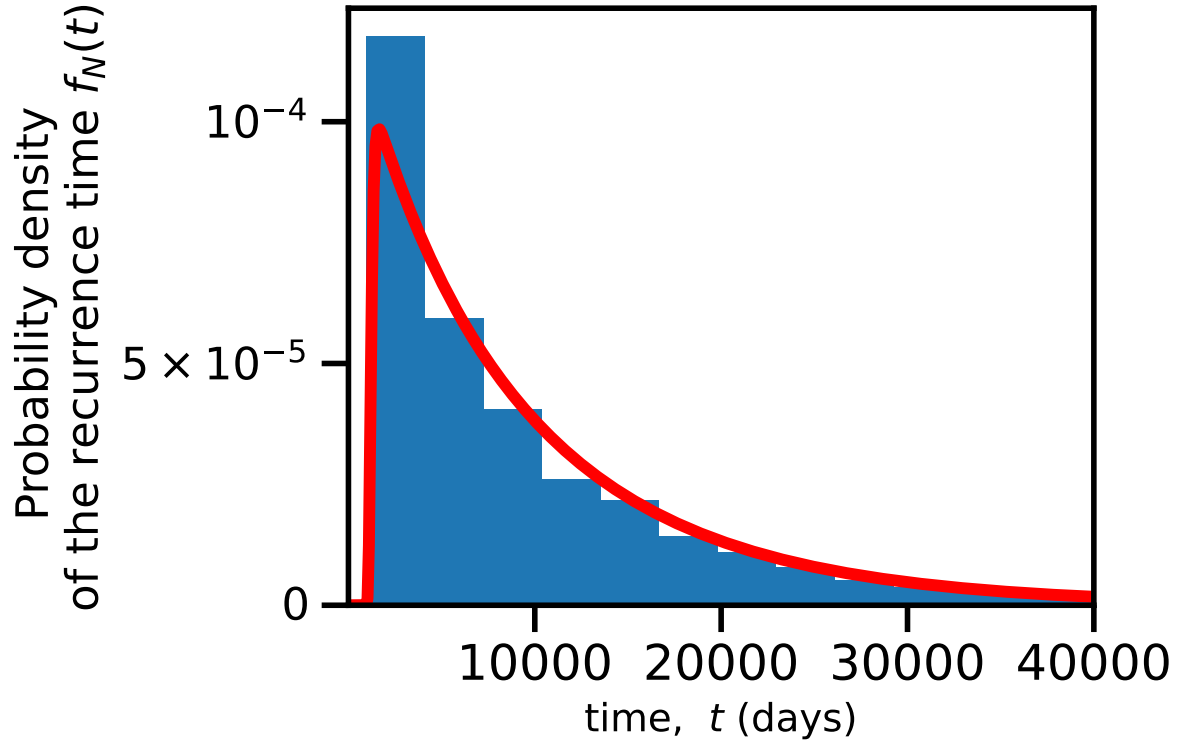


**Figure 11: Distribution of the recurrence time.** Shown is the distribution of the time for the mutant cell population to reach size  $N$ , where  $N$  is the initial number of cancer cells. The red line is analytic result eq. (41) overlaid over the histogram of simulations. Parameters:  $N = 10^6$ ,  $\lambda_w = 0.1$ ,  $\lambda_a = 0.0899$ ,  $\lambda_m = 0.1$ ,  $\mu_w = 0.14$ ,  $\mu_a = 0.09$ ,  $\mu_m = 0.09$ ,  $u = 10^{-2}$ ,  $v = 10^{-7}$ .

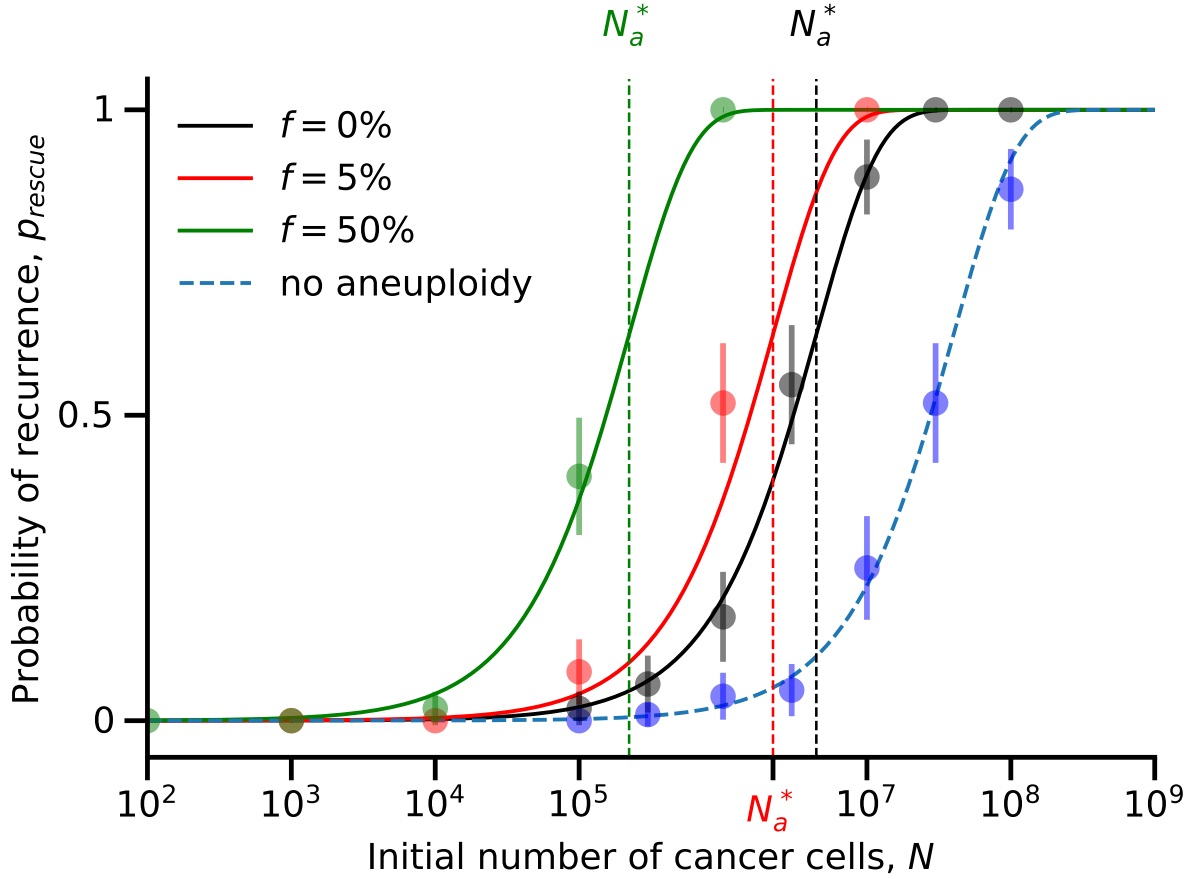


**Figure 12:** The probability of evolutionary rescue (i.e. the probability that the population does not go to extinction),  $p_{\text{rescue}}$ , as a function of the initial tumor size,  $N$ . Dashed vertical line shows the threshold tumor size, above which the probability is very high. Blue dashed line represents the probability of evolutionary rescue as a function of  $N$  without aneuploidy ( $u = 0$ ). The black line represents the case where a fraction  $f = 0\%$  of the initial tumor is aneuploid, the red line represents the case with  $f = 5\%$  and the green line represents the case with  $f = 50\%$ . The dots represent simulations and the error bars represent 95% confidence interval of the form  $p \pm 1.96\sqrt{p(1-p)/n}$  where  $p$  is the fraction of simulations in which the tumor has adapted to the stress and  $n = 100$  is the number of simulations. Parameters:  $\lambda_w = 0.1, \lambda_a = 0.0899, \lambda_m = 0.1, \mu_w = 0.14, \mu_a = 0.09, \mu_m = 0.09, u = 10^{-2}, v = 10^{-7}$ .

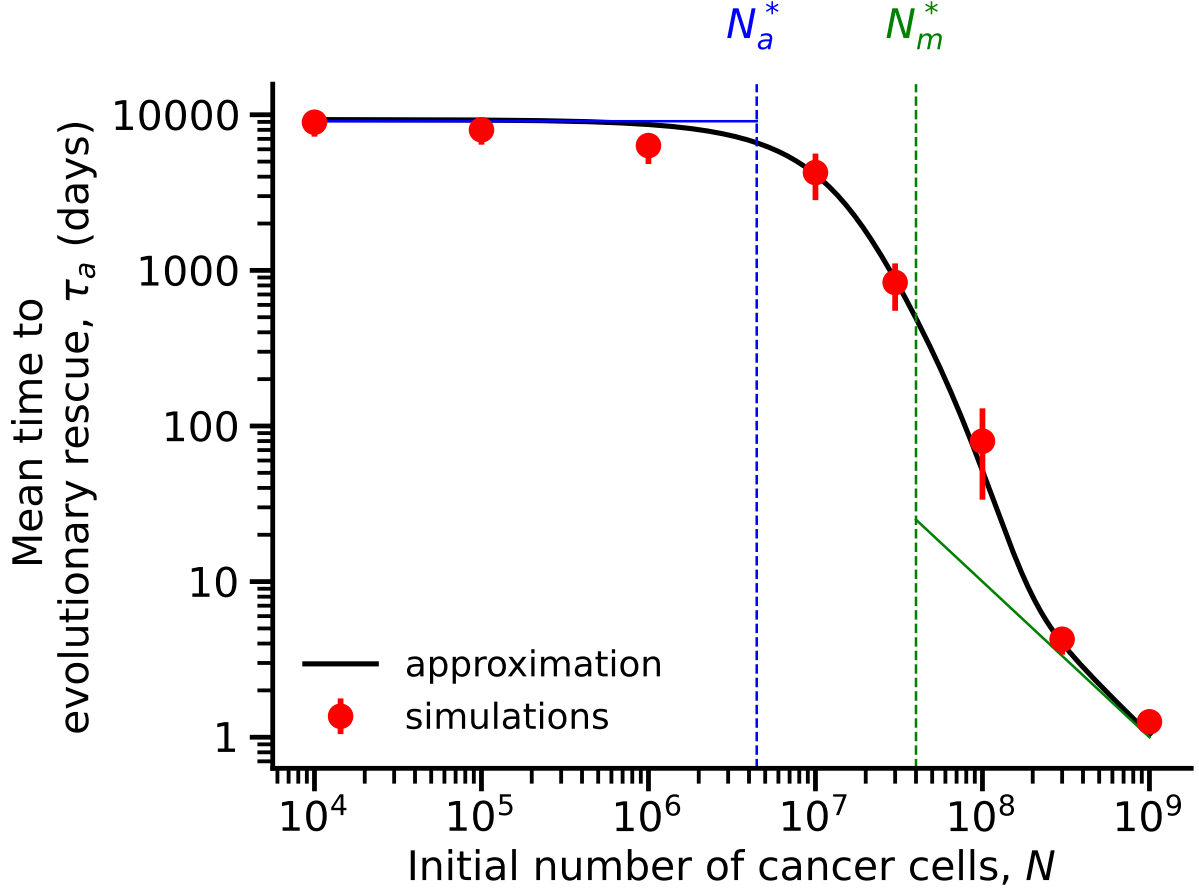


**Figure 13:** Shown is the mean time for appearance of a resistance mutation the leads to evolutionary rescue with aneuploidy ( $u > 0$ ). Our inhomogeneous Poisson-process approximations (solid black lines, right: eq. (28)) is in agreement with simulation results (red markers with 95% confidence intervals obtained with bootstrapping, see Appendix G). Dashed vertical blue line represents the threshold tumor size above which evolutionary rescue is very likely through aneuploidy eq. (4) and the dashed vertical green line represents the threshold tumor size above which evolutionary rescue is very likely through direct mutation eq. (3). Solid lines represents the approximations eq. (8) ( $N < N_a^*$  blue line and  $N > N_m^*$  green line). Parameters:  $\lambda_w = 0.1, \lambda_m = 0.0899, \lambda_m = 0.1, \mu_w = 0.14, \mu_a = 0.09, \mu_m = 0.09, u = 10^{-2}, v = 10^{-7}$ .

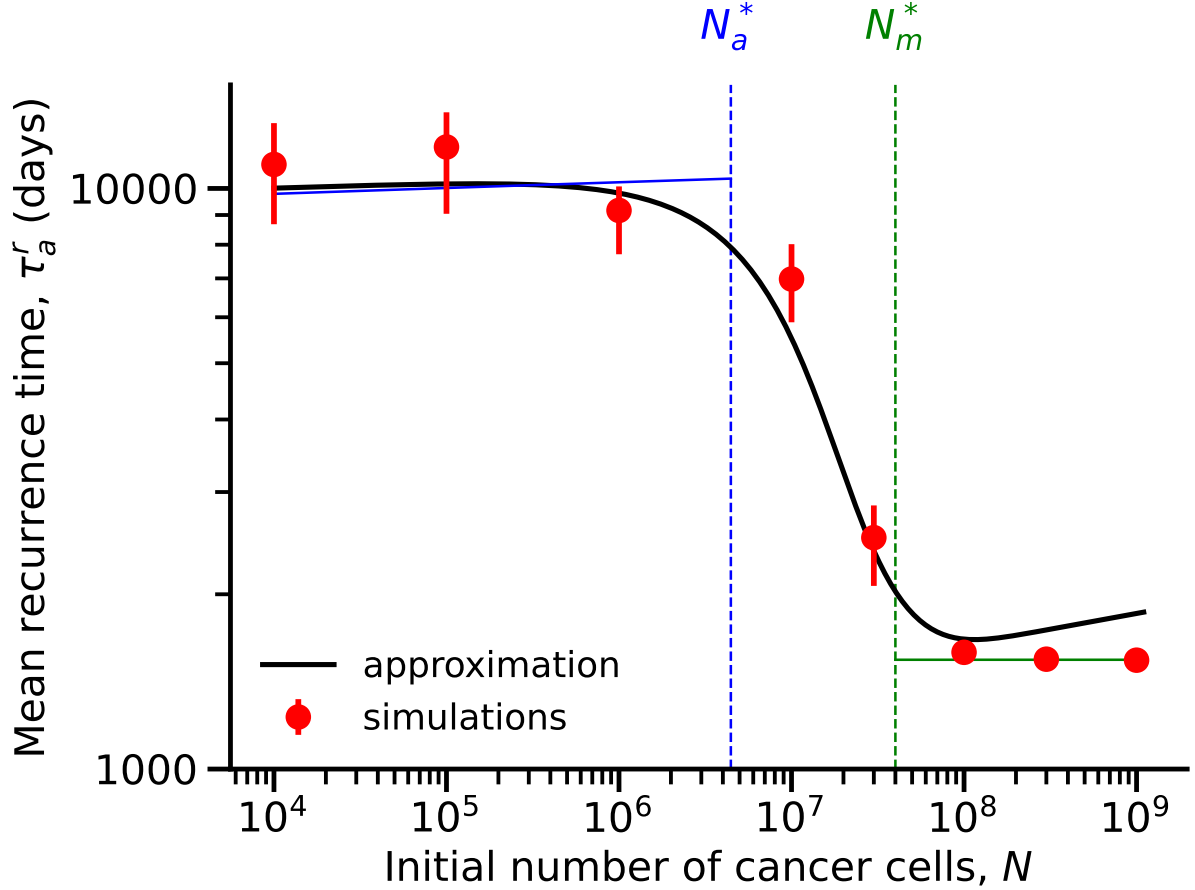


**Figure 14:** The mean time for the mutant cell population to reach size  $N$ , where  $N$  is the initial number of cancer cells. Our inhomogeneous Poisson-process approximation (solid black line, eq. (32)) is in agreement with simulation results (red markers with 95% confidence intervals obtained with bootstrapping, see Appendix G) for small and intermediate values of  $N$ . Dashed vertical blue line represents the threshold tumor size above which evolutionary rescue is very likely through aneuploidy eq. (4) and the dashed vertical green line represents the threshold tumor size above which evolutionary rescue is very likely through direct mutation eq. (3). Solid lines represents the approximations eq. (9) ( $N < N_a^*$  blue line and  $N > N_m^*$  green line). The simulations converge to eq. (35) (green line) for large values of  $N \gg N_m^*$ . Parameters:  $\lambda_w = 0.1$ ,  $\lambda_a = 0.0899$ ,  $\lambda_m = 0.1$ ,  $\mu_w = 0.14$ ,  $\mu_a = 0.09$ ,  $\mu_m = 0.09$ ,  $u = 10^{-2}$ ,  $v = 10^{-7}$ .

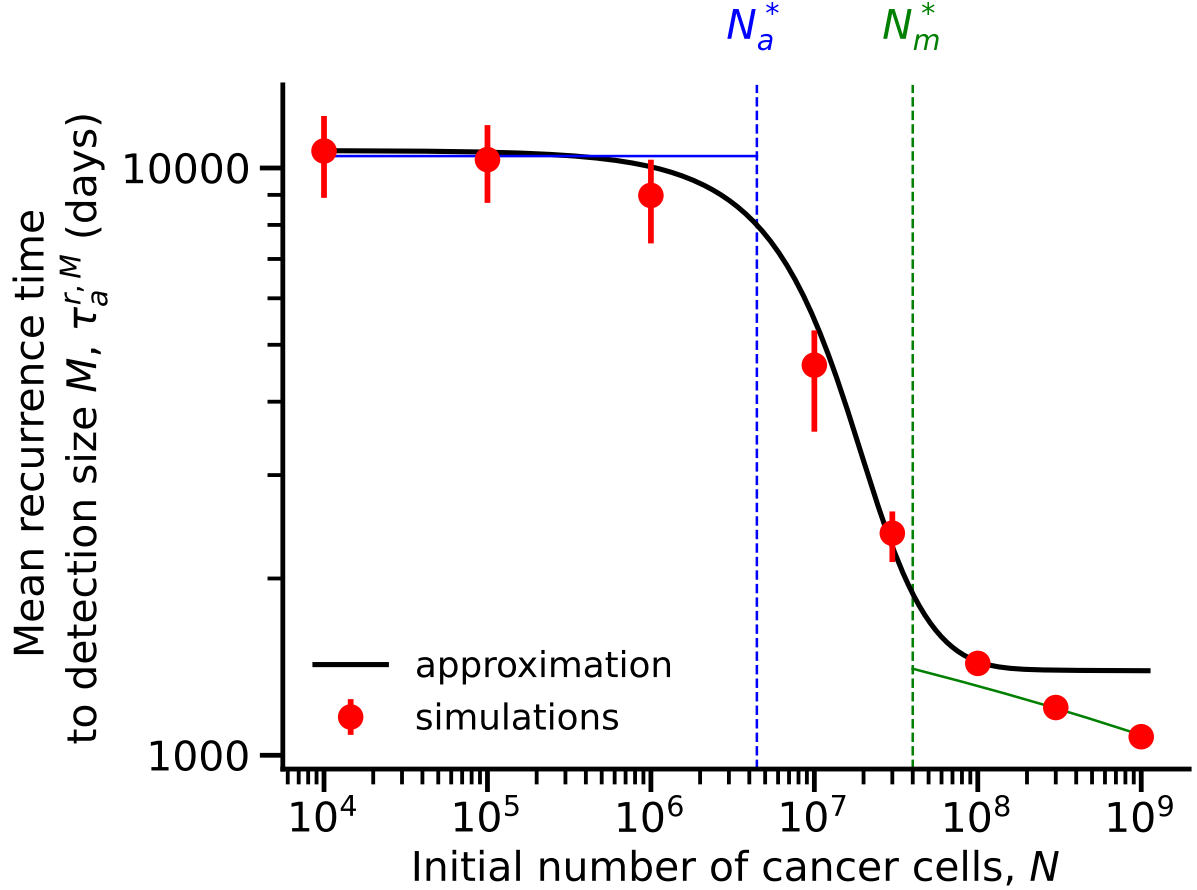


**Figure 15:** The mean time for the mutant cell population to reach size  $M$ , where  $M$  is the tumor detection size. Our inhomogeneous Poisson-process approximation (solid black line, eq. (36)) is in agreement with simulation results (red markers with 95% confidence intervals obtained with bootstrapping, see Appendix G) for small and intermediate values of  $N$ . Dashed vertical blue line represents the threshold tumor size above which evolutionary rescue is very likely through aneuploidy eq. (4) and the dashed vertical green line represents the threshold tumor size above which evolutionary rescue is very likely through direct mutation eq. (3). Solid blue line represents the approximation eq. (36) with  $\tau_a$  from eq. (8) for  $N < N_a^*$  and the solid green line represents the approximation eq. (37) for  $N > N_m^*$ . The simulations converge to eq. (37) (green line) for large values of  $N \gg N_m^*$ . Parameters:  $\lambda_w = 0.1$ ,  $\lambda_a = 0.0899$ ,  $\lambda_m = 0.1$ ,  $\mu_w = 0.14$ ,  $\mu_a = 0.09$ ,  $\mu_m = 0.09$ ,  $u = 10^{-2}$ ,  $v = 10^{-7}$ .

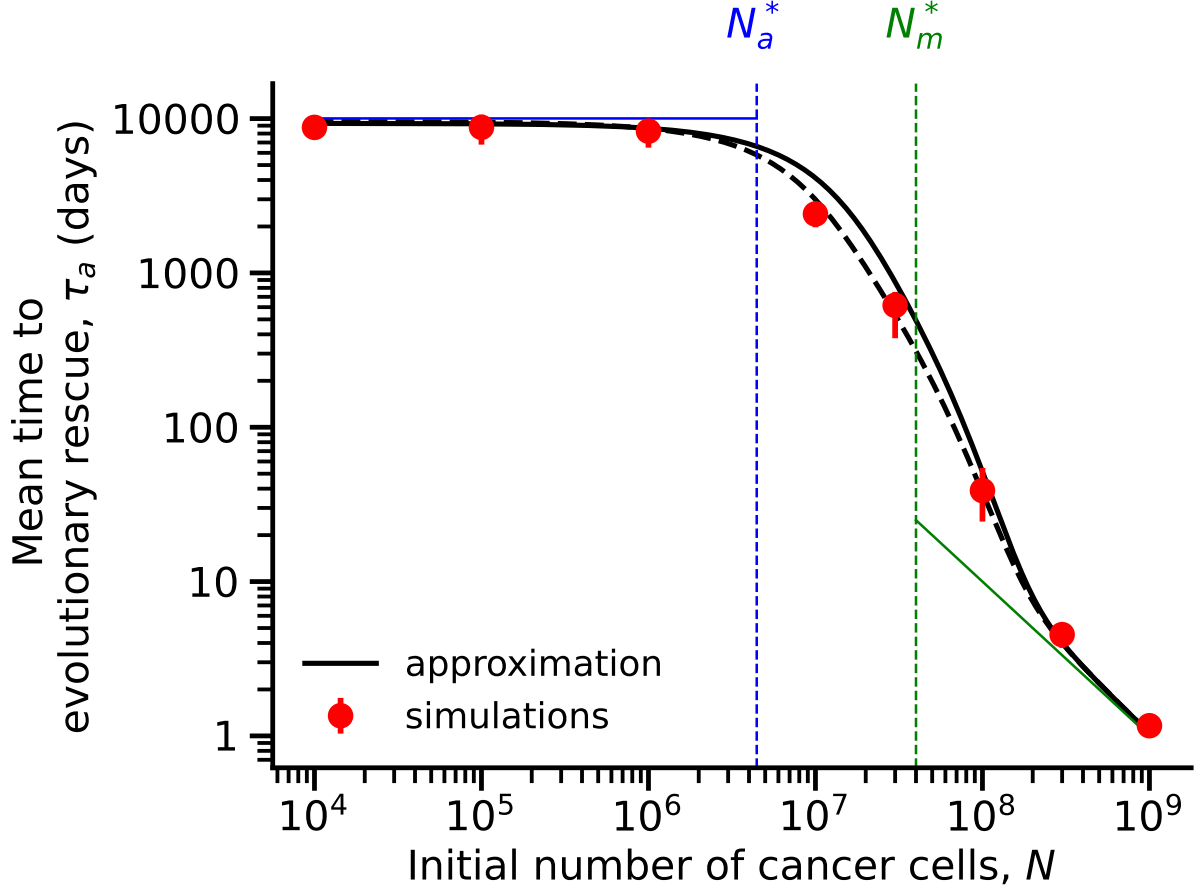


**Figure 16:** Shown is the mean time for appearance of a resistance mutation the leads to evolutionary rescue with aneuploidy ( $u > 0$ ). Black lines represent our inhomogeneous Poisson-process approximations (solid black line, eq. (28); dashed black line eq. (31)). Dashed black line is the inhomogeneous Poisson-process approximation where a fraction  $f$  of tumor is aneuploid at the onset of drug therapy which is in agreement with simulation results (red markers with 95% confidence intervals obtained with bootstrapping, see Appendix G). Dashed vertical blue line represents the threshold tumor size above which evolutionary rescue is very likely through aneuploidy eq. (4) and the dashed vertical green line represents the threshold tumor size above which evolutionary rescue is very likely through direct mutation eq. (3). Solid lines represents the approximations eq. (8) ( $N < N_a^*$  blue line and  $N > N_m^*$  green line). Parameters:  $\lambda_w = 0.1, \lambda_m = 0.0899, \lambda_m = 0.1, \mu_w = 0.14, \mu_a = 0.09, \mu_m = 0.09, u = 10^{-2}, v = 10^{-7}, f = 1.36\%$ .